COEFFICIENT OF FRICTION OF
AIRCRAFT TIRES ON CONCRETE RUNWAYS

ROBERT R. LUTHMAN

UNIVERSITY OF DAYTON

MARCH 1955

AIRCRAFT LABORATORY
CONTRACT No. AF 33(616)-2251
PROJECT No. 1369
TASK No. 13487

SEP 1 2 1955

WRIGHT AIR DEVELOPMENT CENTER
AIR RESEARCH AND DEVELOPMENT COMMAND
UNITED STATES AIR FORCE
WRIGHT-PATTERSON AIR FORCE BASE, OHIO

FOREWORD

This report was prepared by Robert R. Luthman of the Division of Research, University of Dayton, Dayton, Ohio, on Contract No. AF 33(616)-2251, under Project No. 1369, Alighting Gear Components, Task No. 13487, Coefficient of Friction and Wear Tests. The project was administered by the Mechanical Branch, Aircraft Laboratory, Wright Air Development Center, with Mr. Ralph L. Jacob of the Tire Section, Mechanical Branch acting as project engineer.

The author wishes to acknowledge the assistance given by Mr. William A. Hamilton, presently Chief of the Tire Section, as well as the assistance of Mr. Kenton W. Zahrt and Maj Walter J. Klein, while each was serving in this capacity; the support rendered by the personnel of the Technical Photographic Services Units, Wright-Patterson Air Force Base, for time and effort expended in the planning, installing, and servicing of the photographic equipment throughout the test; and especially the cooperation extended by the personnel of the Aircraft Engineering Branch, Directorate of Material, WADC, particularly on the part of Mr. James T. Sharkey, planner, Mr. Bruce W. Baughman, foreman, Mr. Warren A. Henninger, crew chief, and the entire crew. Without the whole-hearted cooperation and assistance of all of these men the project would not have been efficiently completed.

ABSTRACT

The principal objective of the project was the determination of the maximum attainable coefficient of friction under various conditions of velocity and vertical loading. To accomplish the objective, a modified A-20 nose landing gear equipped with a 26 x 6.6 tire, wheel, and brake assembly was mounted on a special test fixture which had previously been installed in the bomb bay of a B-26 taxi-test vehicle. Full scale skid tests were performed on the 10,000 ft concrete runway at Area C, Wright-Patterson Air Force Base. The variation in the coefficient of friction with velocity up to 140 mph was established and is presented herein in graphical form; however, although some variation in the coefficient of friction was noted for various applied vertical loads, no definite relationship was established regarding the instantaneous vertical loads. The results indicate that the coefficient of friction is actually somewhat higher than the value currently used in calculations.

PUBLICATION REVIEW

This report has been reviewed and is approved.

FOR THE COMMANDER:

for

DANIEL D. McKEE
Colonel, USAF
Chief Aircraft Laboratory
Directorate of Laboratories

CONTENTS

Nature and Background

The inception of this program was brought about by the general need throughout the aircraft industry for more accurate information regarding the stopping power obtainable from aircraft tires. This stopping power is comprised, not only of the frictional forces developed between the tire and the runway, but also of those forces required to shear off the small bits of tread rubber squeezed into the pores of the concrete. Throughout this report both effects will be included in the term "friction," and the "coefficient of friction," as usual, will be understood as being the quotient of the total horizontal forces divided by the existing vertical load.

The need for an accurate value of the coefficient of friction of aircraft tires on concrete runways, as well as its variations under prescribed conditions, is experienced primarily by three branches of the industry. First, those people engaged in the design and manufacture of air-frames and landing gears can perform their function accurately and effectively only if they have reliable information available regarding all of the phenomena which enter into their considerations. Second, the knowledge of the coefficient of friction and its variations is of great importance in transforming the results of any experiments involving landing gears, wheels, brakes, or tires which may be performed in a laboratory into more realistic values for use in field applications. Finally, a third use for which the information may be of vital importance is in the establishment of design criteria for tires to be used on present or future aircraft with high landing speeds.

Several previous attempts to measure the coefficient of friction have been made by the Aircraft Laboratory of the Wright Air Development Center. The first of these, which was the only one carried to completion, was conducted in 1947 by the strain gage instrumentation of one of the main landing gears of an A-20 aircraft from which the outboard wing sections had been removed for taxi-test purposes. The results of this attempt were published in the Memorandum Report No. MCREXA6-45257-4-1 entitled "Tests for Determining the Coefficient of Friction of 44 in. Smooth Contour Tires on Concrete Runways." These results appear to be inconclusive, for it was noted in the "conclusion" of the report that the values of the coefficient at the time of pending skid were rather erratic and were not plotted. Since these are the points at which the coefficient reaches its highest value during a skid, it is reasonable to assume that the results, as reported, are somewhat lower than the values actually encountered. Also, in this first test, variations of the parameters involved were restricted by the limitations of the test vehicle. Eventually the problem was presented to the Division of Research of the University of Dayton, and an initial attempt to obtain the required information was made by instrumenting the left main landing gear of a B-26 taxi-test vehicle. During this attempt, it was found that the geometric configuration of the landing gear was such that satisfactory locations for the strain gages could not be found. Nearly all of the strain gages installed exhibited such high responses to at least two of the three primary loads, viz. vertical, drag, and side, that an accurate determination of those loads was impossible. It was then decided to continue the program using an auxiliary wheel suspended

from the bomb bay of the vehicle in such a way that the measurements could be made with satisfactory accuracy.

Scope of Program

There are numerous factors affecting the value of the coefficient of friction, the most important of which are the composition and surface conditions of the runway, tire tread design and tread rubber composition, vertical load, tire deflection, and the velocity of the test vehicle. In order to render some of the parameters ineffective, it was decided to use tires of the same tread design and, if possible, by the same manufacturer, to conduct the skid tests, whenever practical, on the same runway, and to skid only when the runway was dry. The investigation of the remaining parameters of velocity and vertical load comprise the scope of the program. The effect of vertical loading was to be determined by conducting skids with initial applied loads ranging in 1000 lb increments from 5000 to 8000 lb. For each increment of applied load the skids were to be performed at velocities of from 50 to 150 mph in approximately 15 mph increments.

Objective

The objective of the program was to measure the maximum coefficient of friction attainable between aircraft tires and concrete runways under various conditions of vertical load and velocity and to determine the variations in the coefficient, if any, with these parameters.

SECTION I

PROCEDURE

1.1 General

One of the most difficult problems associated with nearly any attempt to make coefficient of friction measurements is the accurate determination of the normal and horizontal forces. Since the horizontal force experienced by a tire during a skid is the vectorial sum of the side and drag loads, they, together with the vertical load, constitute the three primary measurements which were involved. Consequently, the general procedure which was outlined for the program embodied the design, installation, and instrumentation of a theoretically ideal structure which would permit the satisfactory determination of these loads.

1.2 Vehicle

The vehicle used for the skid tests was a B-26 aircraft from which the outboard wing sections had been removed. The vehicle is shown in Fig. 1. A special fixture, which had been designed by the Bendix Aviation Corporation for a series of nose wheel shimmy tests, was installed in the bomb bay. It was comprised chiefly of a hydraulically operated, elevator-like carriage within a heavy framework bolted to the wing spars. The main function of the fixture was to provide a means of varying the vertical load on a test tire. A wheel and brake assembly was mounted on a modified A-20 nose gear which was affixed to the carriage through appropriate load cells and mounts. The lower portion of the assembly is shown in Fig. 2 and a cut-away schematic of the entire fixture in Fig. 3. For the skids, 14 ply rating, nylon, type VII, tires were used because of their general use on a number of operational aircraft and their availability.
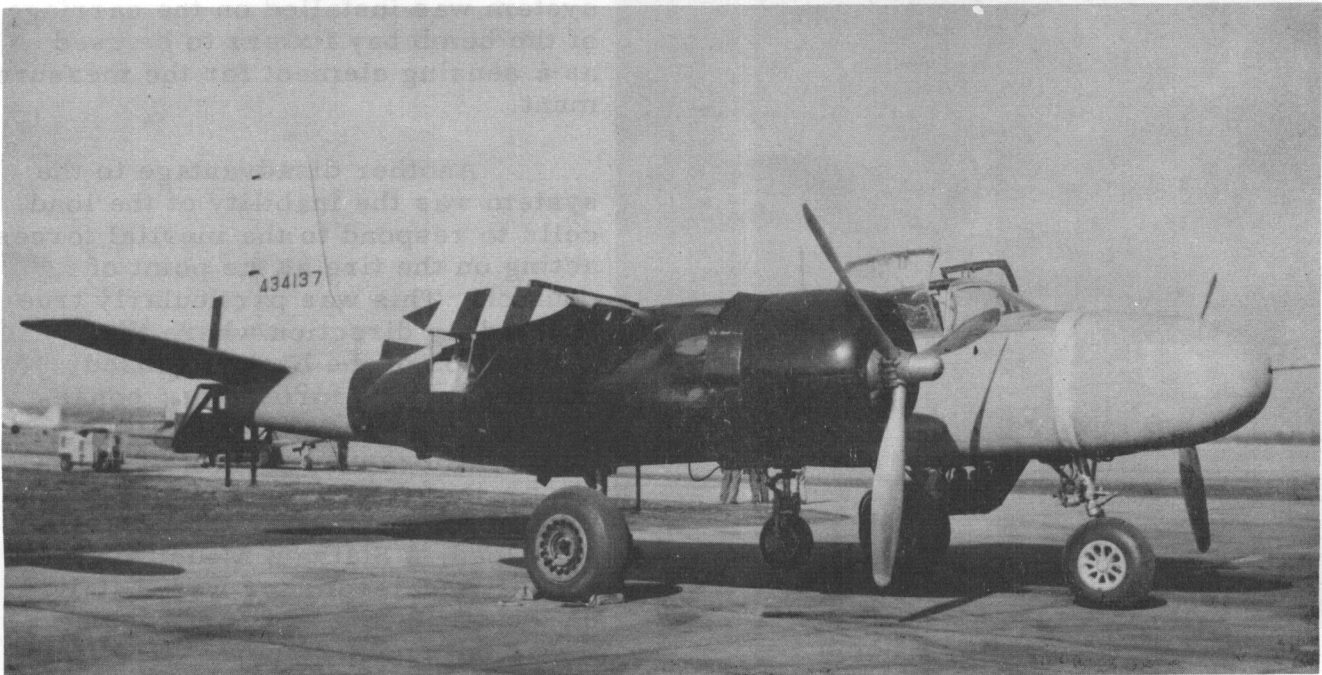
Fig. 1 B-26 Taxi-Test Vehicle

1.3 Instrumentation

The instrumentation of the vehicle consisted of the installation of all of the equipment necessary to measure and record the instantaneous values of all parameters which were considered to be of possible influence in the determination of the coefficients of friction existing during the skids. With the exception of the details of the bomb bay fixture, which are shown in Fig. 3, the complete installation is presented schematically in Fig. 4. The principal components of the entire system were those directly related to the measuring and recording of the desired data. These consisted of sensing elements, by which were developed electrical outputs proportional in magnitude to the quantities being measured, and of an oscillograph utilizing current-sensitive galvanometers and light-sensitive paper for the continuous recording of these output signals.

As sensing elements for the measurements of the vertical, drag, and side loads, Baldwin-Lima-Hamilton, type U-1 Load cells were used. From the cell locations, Fig. 3, it can readily be seen that the drag and side loads could be determined by taking the algebraic sums of the upper and lower cell responses in their corresponding directions. The vertical load would, of course, be proportional to the output of the single cell in the vertical direction.

Since the load cells were aligned in directions parallel and perpendicular to the strut center line, they could respond only to those components of the existing forces which were in these directions. This condition was considered to be relatively important for the vertical and drag load determination, since no simple means could be found to control adequately the fore and aft pitching of the vehicle during the skid runs. Consequently, it was decided to measure the angle of pitch, or attitude, of the vehicle and apply an analytical correction to these two quantities. For this purpose, the vertical gyro component of an E-6 autopilot system was installed on the carriage of the bomb bay fixture to be used as a sensing element for the measurement.

Another disadvantage to the system was the inability of the load cells to respond to the inertial forces acting on the tire at the point of contact. This was particularly true in the drag direction where the application of the brakes caused rapidly varying forces and, consequently, high accelerations. As a means of measuring these accelerations, and hence of providing a method for correcting the measured drag load, a Statham Model A-18 Linear Accelerometer was installed on the strut, Fig. 5. Also, since it was not known in advance whether or not the deceleration of the entire vehicle, due to the skidding of the

Fig. 2 Lower Portion of Bomb Bay Fixture Showing Test Wheel and Strut
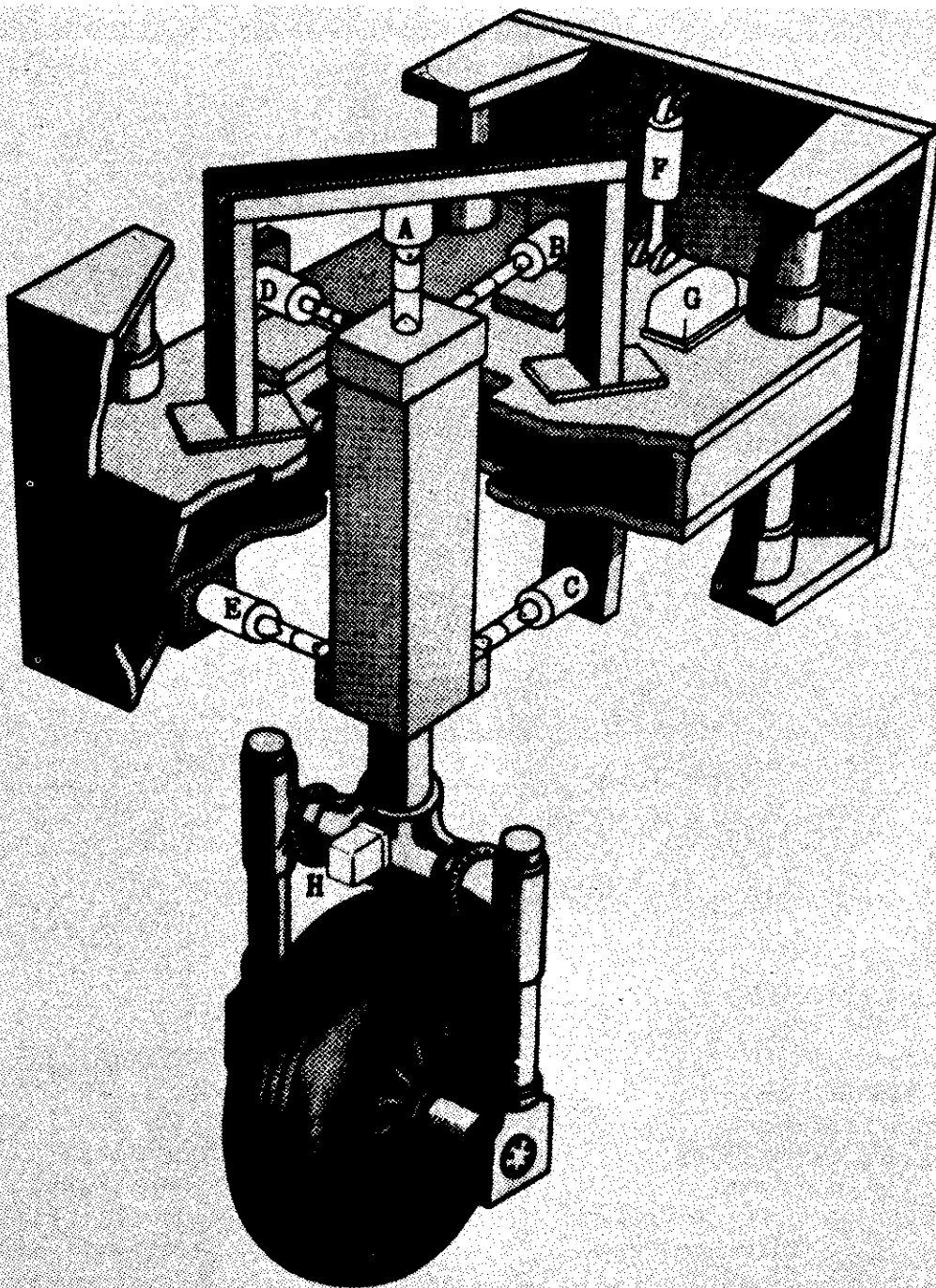
A Vertical Load Cell
B Upper Drag Load Cell
C Lower Drag Load Cell
D Upper Side Load Cell

E Lower Side Load Cell
F Carriage Operating Cylinder
G Pitch Angle Gyro
H Accelerometer

Fig. 3 Cut-away Schematic View of Bomb Bay Fixture
Showing Load Cells and Their Locations

A—Pilot's Seat
B—1000 fps Camera
C—128 fps Camera
D—Auxiliary Power Unit
E—Bomb Bay Fixture
F—Vertical Gyro Power Supply
G—Hydraulic Components Panel
H—Converter
I—Pulse Generator Power Supply
J—Timing Pulse Generator
K—12v Battery
L—Bridge Balance
M—Electrical Control Panel

N—Oscillograph
O—Ass't Technician's Seat
P—C. G. Accelerometer
Q—Test Wheel
R—Ground Speed Aux Wheel
S—Hydraulic Pump
T—Plexiglas Viewing Panel
U—24v Batteries
V—Hydraulic Control Panel
W—Timing Pulse Micro-Switch
X—Technician's Seat
Y—Brake Lever

Fig. 4 Drawing of Taxi-Test Vehicle Showing Locations of
Instrumentation and Control Components

test tire, would be appreciable and would have to be subtracted from the measured strut-acceleration, another similar accelerometer was mounted near the center of gravity of the vehicle.

A correction was also necessary to compensate for the deflection of the test gear when under the influence of a drag load and the resulting eccentric vertical loading condition. The correction is explained in detail in par. 2.3.2 of the Appendix to this report.

In addition to the above, two other measurements were made. For the determination of the velocity parameter being investigated, the ground speed of the vehicle was measured by recording the output of a tachometer generator coupled, through a pulley arrangement, to an auxiliary wheel which was free to roll along the ground. The entire device is shown in Fig. 6. Also, the radial speed of the test wheel was measured and converted to peripheral speed for the determination of the relative velocity between the tire and runway. The measurement was made by means of a contactor device on the test wheel as shown in Fig. 7. It was so arranged that three blades, protruding from the thermal expansion slots in the brake disc, made contact with a wiper on the torque flange of the axle at three equal intervals during each revolution, and the corresponding pulses were impressed on an oscillograph galvanometer.

One oscillogram trace was also provided for recording a timing signal pulse for coordination between the oscillographic data.
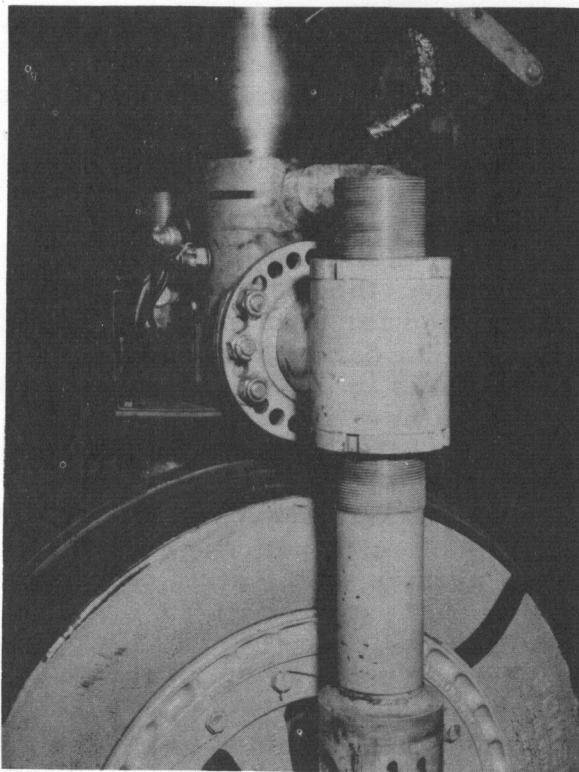
Fig. 5 Close-up of Strut
Accelerometer Installation
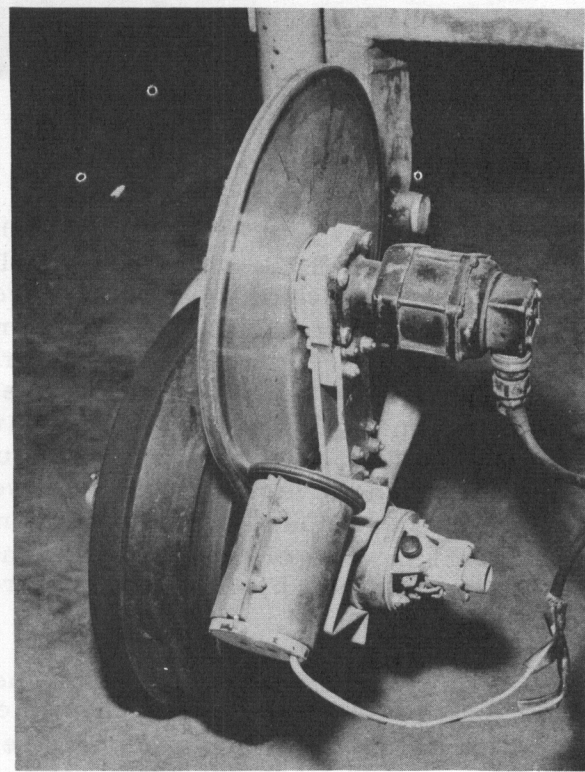
Fig. 6 Close-up of Ground Speed
Wheel and Tachometer

1.4 Photography

High Speed motion picture coverage was provided by the Technical Photographic Service Unit of WPAFB for the purpose of supplementing the oscillographic data. Two cameras were installed as shown in Fig. 8. One was an Eastman B1A with a speed of 128 frames per second, and the other was an Eastman High-Speed operating at approximately 1000 frames per second. Both were equipped with timing lights synchronized with the timing pulse on the oscillograph.

The sides of the test tires exposed to the camera were painted white with the exception of two radial strips which were left black to accentuate the appearance of wheel rotation.

1.5 Operational Procedure

In order to evaluate properly the effects of vertical load and velocity on the maximum coefficient of friction attainable during a skid, a complete sequence of skids was scheduled for each of four applied

Fig. 7 Contactor Device for Wheel Speed Measurement

vertical load settings, viz. 5000, 6000, 7000, and 8000 pounds. Each sequence included a set of three skids at each 15 mph increment of velocity from 50-140 mph plus two additional skids at approximately 150 mph, the highest speed attainable by the vehicle. The tire pressure was varied for each of the applied vertical loads such that the characteristic section height deflection of 32% for Type VII aircraft tires was maintained. The three skids in one set were performed in succession during a single pass down the runway, a new tire being used for each set. All of the skids were conducted at Area C, WPAFB using the 10,000 foot runway whenever possible. However, due to exceedingly heavy traffic, a few of the lower speed skids were conducted on a taxi strip. Both the runway and the taxi strip were of standard air-entrained concrete design with the desired roughness obtained by dragging the fresh concrete surface with a strip of burlap cloth.

The daily procedure established for the skidding phase of the program called for making two passes down the runway, thus completing two sets of skids. Just prior to the first set a procedure was followed during which oscillograph records were taken to determine the "zero" (no load) positions of the oscillogram traces. Also, in order to establish the sensitivities of the various traces for the first set, "cal step" records were taken in which the same unbalances used during the calibration procedure, par. 2.2 of the Appendix, were introduced into the channels. The existing pitch angle at the time of balancing and the initial
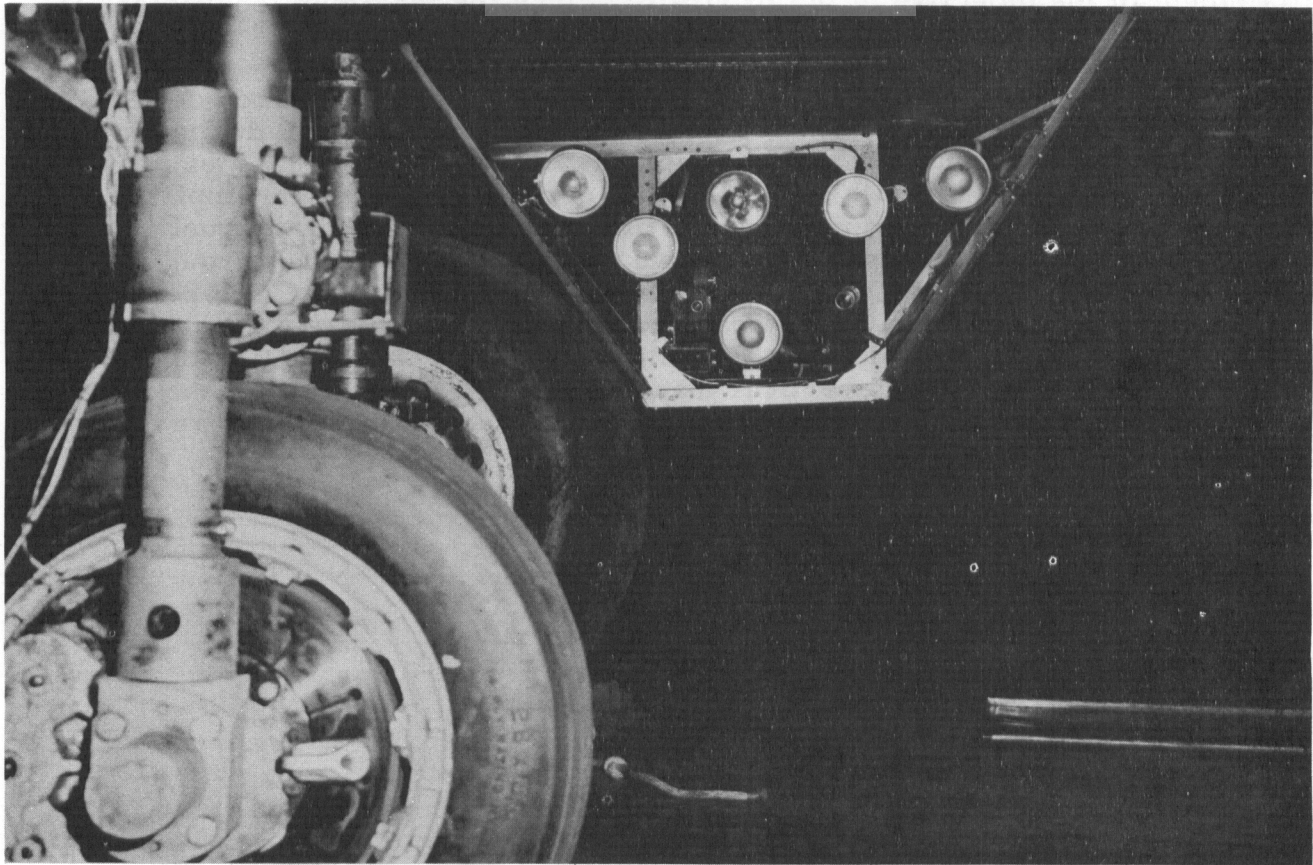
Fig. 8 Camera Installation Below Left Engine Nacelle

tire pressure were also measured and recorded. The initial vertical loading was applied hydraulically at the end of the runway using the vertical load trace deflection, as observed on the oscillograph viewing screen, and a predetermined scale as an indication of magnitude. A "runway zero" record was taken in order to record the applied load. The vehicle was then taxied down the runway stabilizing at the desired speed, at which time the technician in the aft compartment applied the brakes on the test wheel. Since in viewing the wheel from directly behind it, the technician could not always tell when it was completely locked because of the smoke, he released the brakes after approximately two seconds, rather than hazard a blow-out on each run. Preliminary skids indicated that the best results could be obtained when the time duration of the partial skid was from 0.7 to 0.9 second. Consequently, in trying to adhere to this procedure, complete skids were not obtained for all attempts and some had to be repeated. No special attempt was made to hold the complete skid for any definite period of time. After the first set of skids was completed, the vehicle was returned to the ramp, the final tire pressure measured, the tire changed, and, after appropriate zero records, the second set was conducted. Following these, another group of "zero" and "cal step" records were taken for use in the reduction of the test records obtained during the second set of skids.

1.6 Data Reduction

The reduction of the skid data and the ensuing analysis were restricted, in general, to that portion of the data which was directly involved in the

attainment of the objective of the program. Since the maximum coefficient of friction exists at the point of pending skid, the oscillograms were read only throughout that interval of time prior to the locking of the wheel within which the maximum value would be attained. Individual oscillogram trace deflections, from a static reference trace, were measured each 0.01 second during the interval and converted to the proper units of the phenomena being measured. These conversions along with the applicable corrections were accomplished by the use of IBM computing equipment. A time-history curve of the coefficient of friction throughout each skid was drawn by smoothing a curve through all of the measured values of the coefficient attained during the skid. The peak value of the curve was then taken as the maximum value attainable for that particular set of parameters and was used in the determination of the variation of the coefficient with velocity and vertical load. Detailed explanations of the data reduction procedure and the theory behind the corrections involved are presented in Appendix III.

RESULTS

2.1 General

The principal results obtained from this project were the measurements of the maximum coefficients of friction existing during each skid and the variation of the coefficient with velocity. No definite relationship was obtained regarding the coefficient variation with vertical load within any given sequence of skids. However, as the applied loads and tire pressures were increased for the four sequences of skids, a general reduction in the maximum coefficient obtainable was observed. The results will be presented in the order in which they were obtained to indicate the procedure followed in progressing from detailed data to generalized data.

To facilitate rapid identification of the results from the numerous skids performed, a simple code was devised. The first digit in the code indicates the applied vertical load in thousands of pounds, the next three digits indicate the intended velocity at the time of skidding, and the last digit, separated by a hyphen, is the number of the skid in the set. The last digit is greater than three only when a second set of skids was necessary because of not attaining complete skids or because the proper velocity was not achieved during the first set of three skids. Thus a code number of 6110-3 would indicate the third skid in the set conducted with an applied vertical load of 6000 pounds and at an intended velocity of 110 mph.

2.2 Coefficient of Friction vs. Time

Of approximately 100 skids attempted 86 yielded information from which the time history plots of the coefficient of friction could be drawn. All exhibited the same general shape with the measured coefficient increasing from that due to the rolling resistance of the tire to a maximum occurring at the so-called "point of pending skid" just prior to the locking of the wheel.

Several factors affected the individual appearances of the curves among which were, the speed of brake application, high strut accelerations in the aft direction and rapid variations in the vertical load during the skids. Slow braking resulted in comparatively flat time history curves, whereas the other factors resulted in the appearance of scatter, or dispersion, on the curves. In general, all affected the reliability with which the maximum coefficients attained during the skids could be determined. Accordingly, quality ratings were assigned to the individual curves in order that proportionate weights could be considered in the ensuing analyses. The ratings assigned were those of very good, good, fair, and poor.

Some time histories through the points of pending skid are shown in Figs. 9 through 12. These particular skids were chosen to portray the typical appearances of the four qualities of coefficient time history curves. It may be noted on these curves that the degree of certainty with which the maximum values can be determined decreased with the quality rating. The maximum coefficient attained during each skid is presented, along with other pertinent
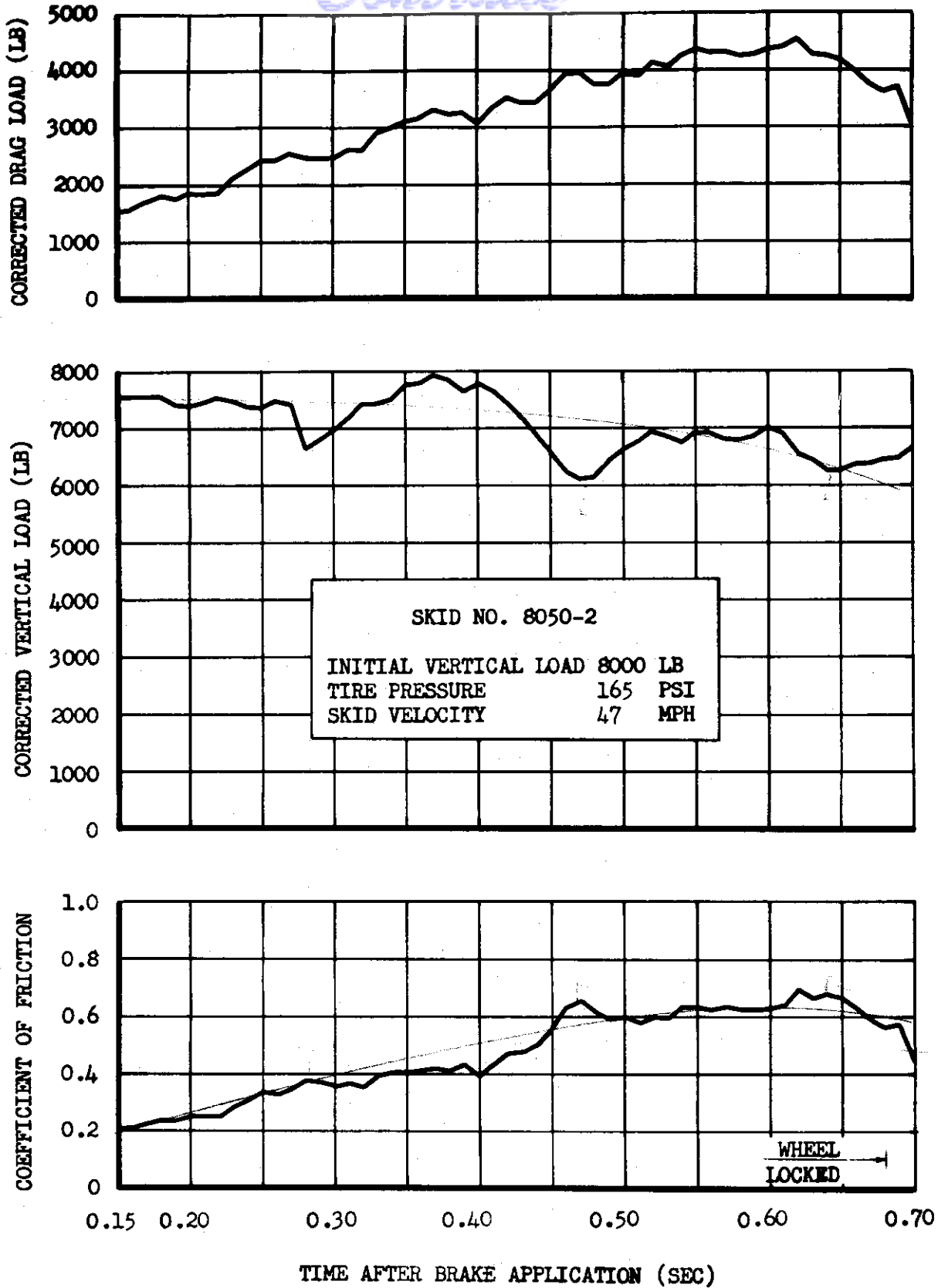
Fig. 9 Coefficient of Friction vs. Time, Skid No. 8050-2 at 32% Tire
Deflection, Quality Rating "Very Good"
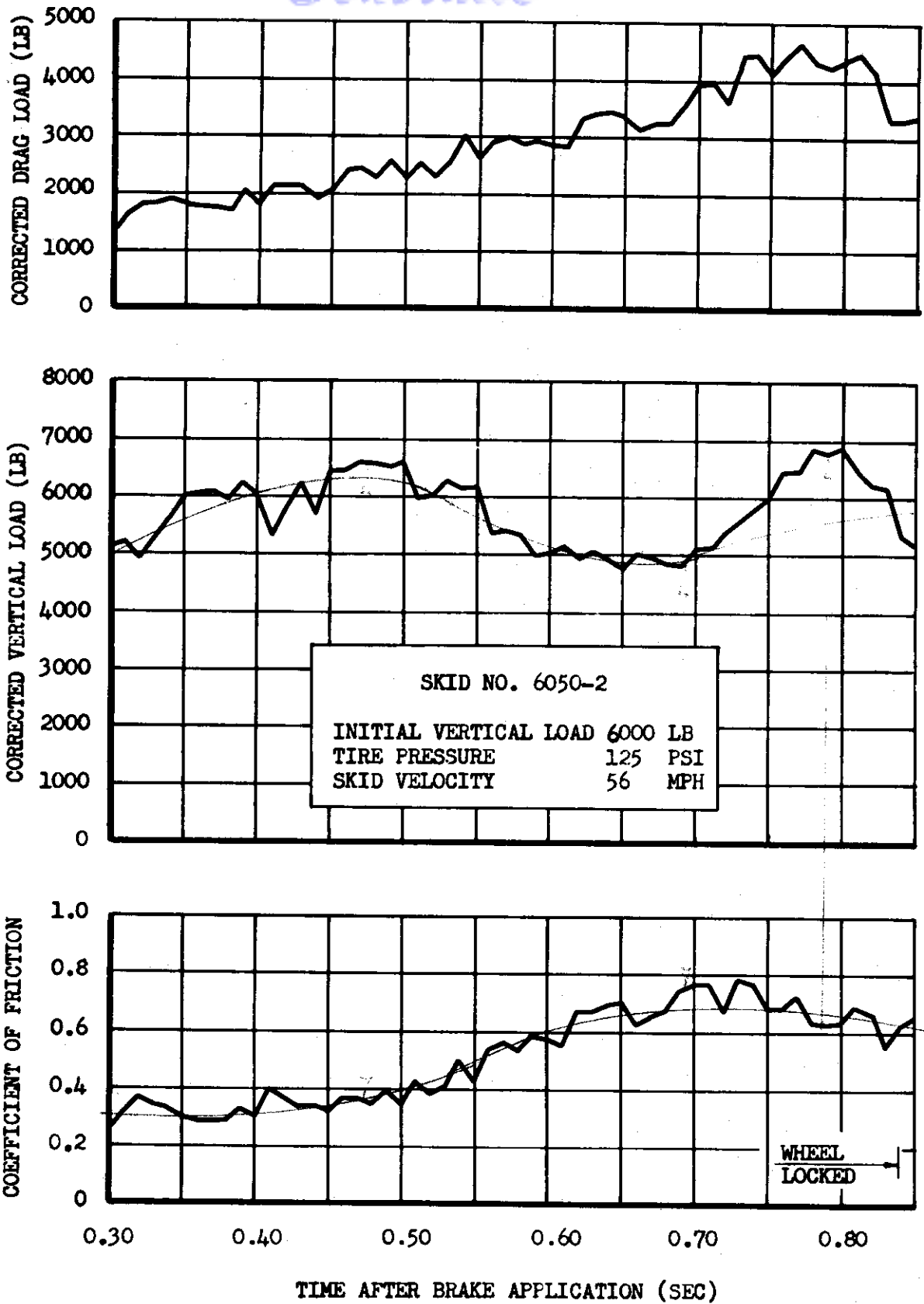
Fig. 10 Coefficient of Friction vs. Time, Skid No. 6050-2 at 32% Tire
Deflection, Quality Rating "Good"
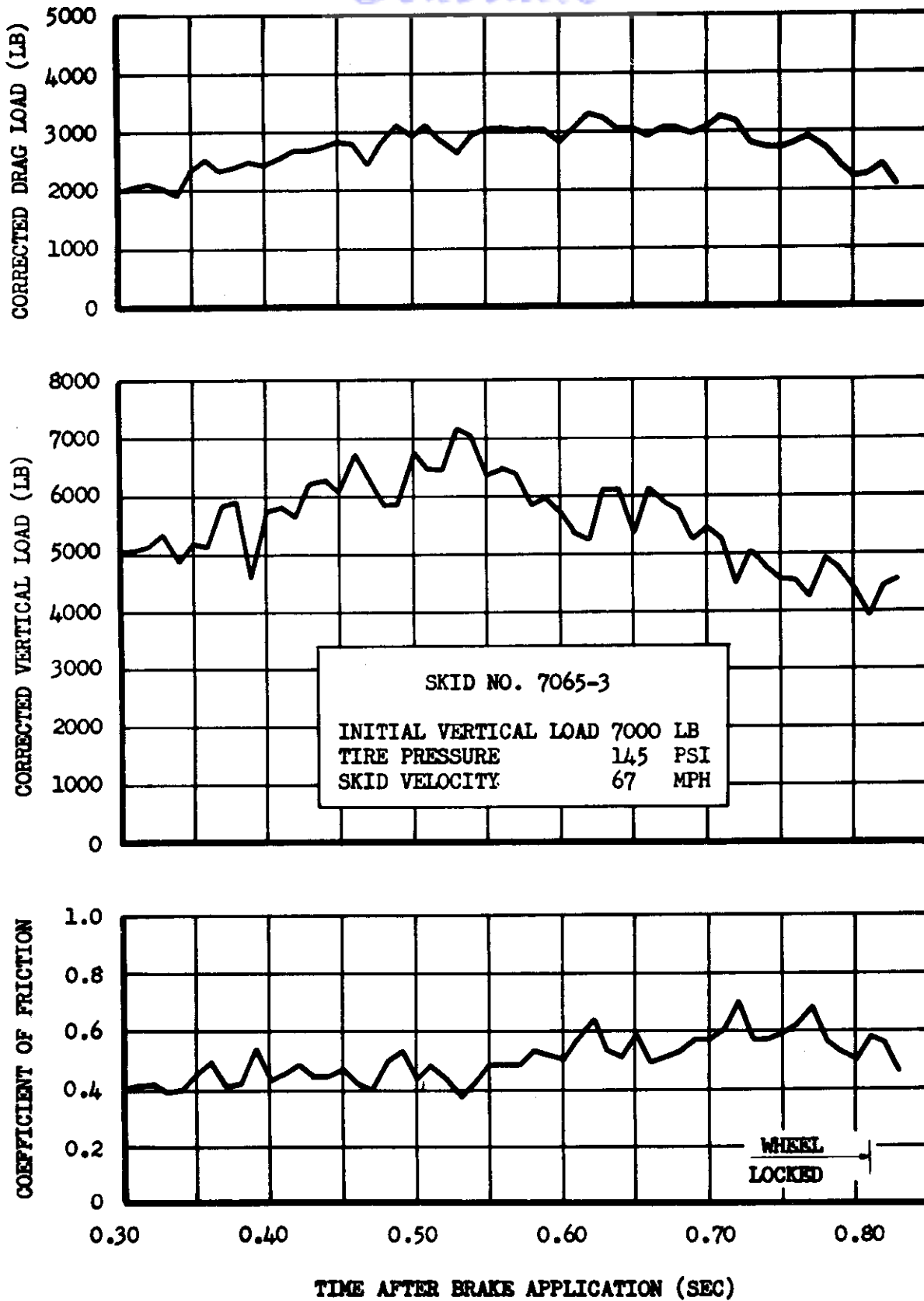
Fig. 11 Coefficient of Friction vs. Time, Skid No. 7065-3 at 32% Tire Deflection, Quality Rating "Fair"
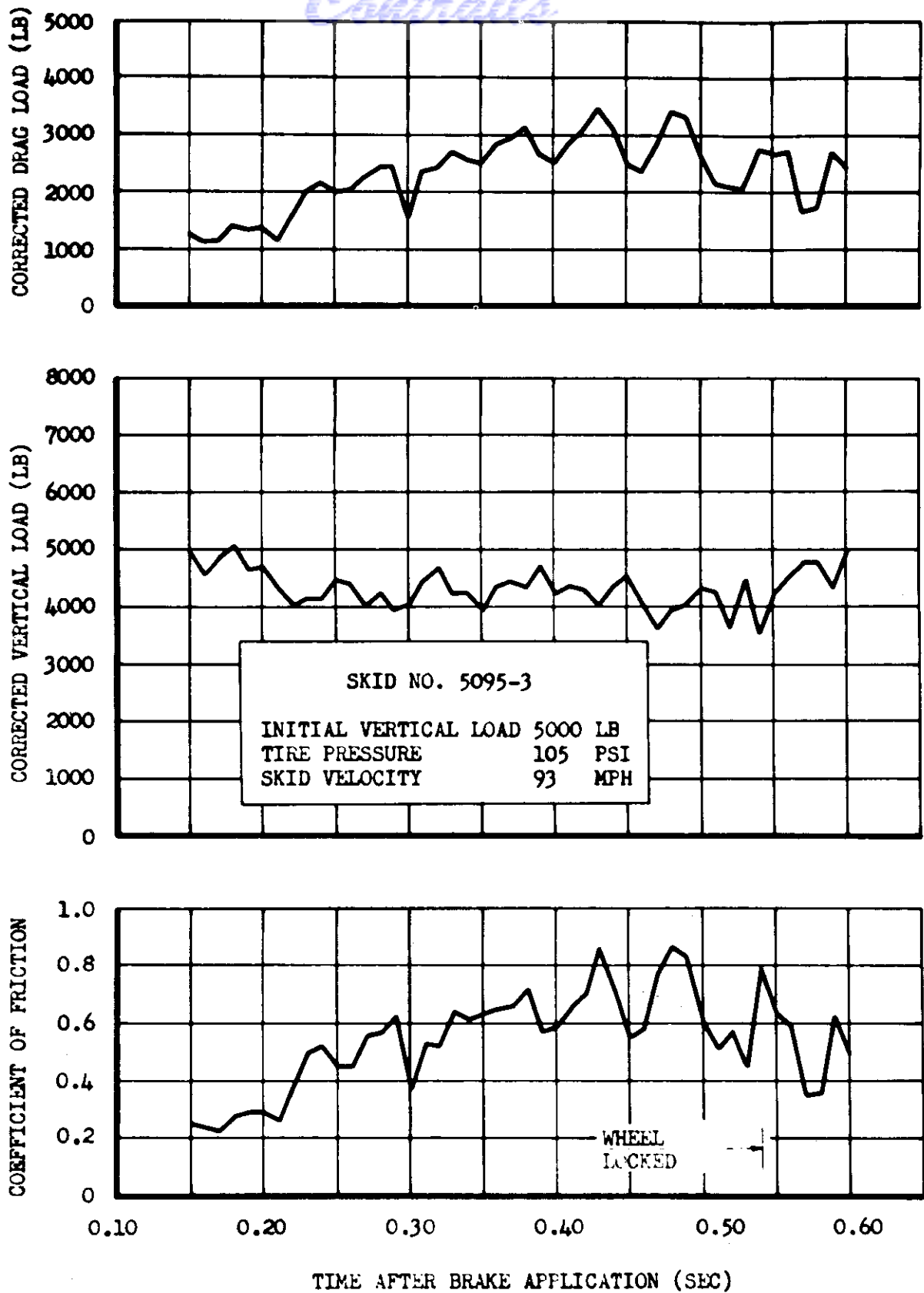
Fig. 12 Coefficient of Friction vs. Time, Skid No. 5095-3 at 32% Tire
Deflection, Quality Rating "Poor"
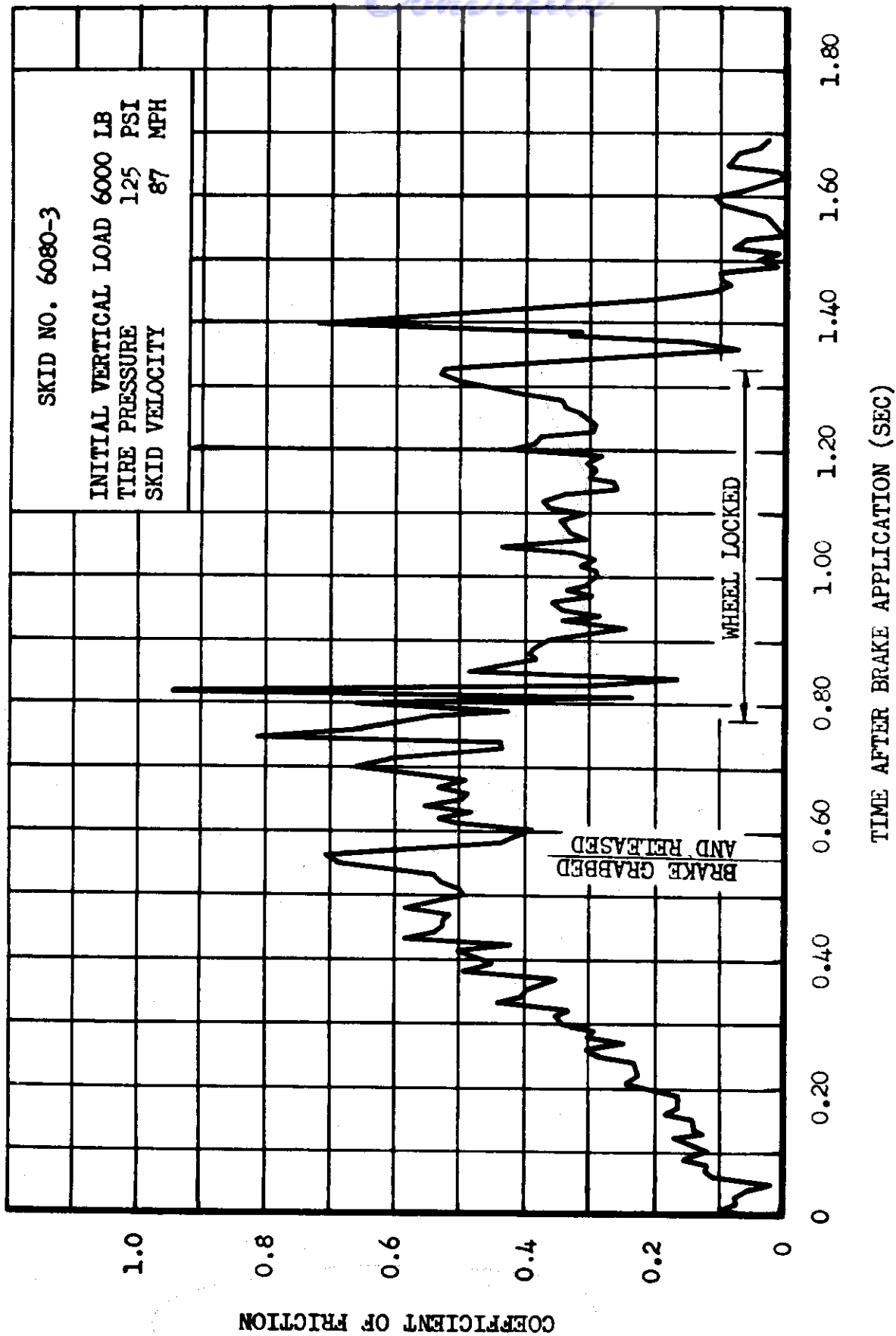
Fig. 13 Coefficient of Friction vs. Time Curve Throughout Skid No. 6080-2 at 32% Tire Deflection

SKID NO. 6080-3

INITIAL VERTICAL LOAD	6000	LB
TIRE PRESSURE	125	PSI
SKID VELOCITY	87	MPH

TIME AFTER BRAKE APPLICATION (SEC)

COEFFICIENT OF FRICTION

WHEEL LOCKED

BRAKE GRABBED AND RELEASED

data, in tabular form in Appendix IV. Also presented in the Figs. 9 through 12 are the time histories of the vertical and drag loads resulting from the application of the corrections described in par. 1.3 of the preceeding section. The Corrected Drag Load curves exhibit the same general shape as those of the coefficients, increasing with time after the brakes were applied. The Corrected Vertical Load curves, on the other hand, although varying through fairly wide limits, showed no general pattern whatsoever. A consideration of the effects of these variations is presented in par. 3.5 of the following section.

Two additional time history curves are shown in Figs. 13 and 14. The first illustrates the variation in the coefficient throughout a complete skid. As can be seen, the coefficient tended to stabilize during the time in which the wheel was completely locked. On this particular skid the brake locked instantaneously at 0.57 second, showing a peak just prior to this time. This preliminary locking of the test wheel was not normal, however, and the preceeding peak was disregarded in favor of the value of 0.52 at 0.65 second which followed more closely the pattern established on the majority of skids.

Fig. 14 shows the variation in the coefficient of friction under the condition of zero relative velocity between tire and runway. The test was performed to determine the static coefficient of friction for the same conditions under which the actual skids were run, with the exception of the dynamic effects. The curve shows the maximum static coefficient attained under these conditions to be 0.83. The rapid decline in the curve after the

SKID NO. 6000-1

INITIAL VERTICAL LOAD 6000 LB
TIRE PRESSURE   125 PSI
SKID VELOCITY   0   MPH
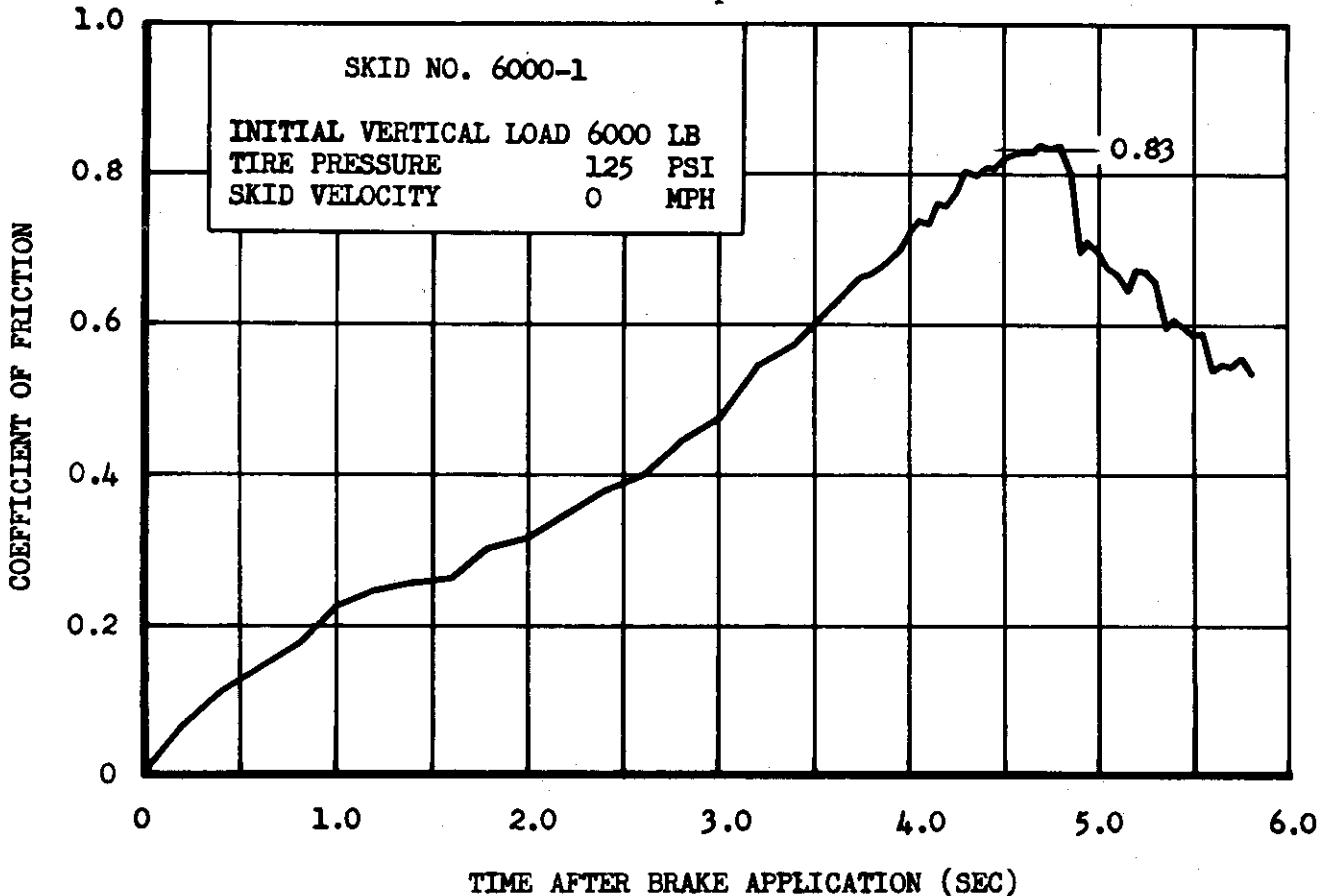
Fig. 14 Coefficient of Friction vs. Time, Skid No. 6000-1 at 32% Tire Deflection, Showing Static Coefficient to be 0.83

WADC-TR-55-179   15

2.3 Coefficient of Friction vs. Velocity

For the determination of the variation in the coefficient of friction as a function of velocity, the maximum coefficients attained during the individual skids were plotted against their skid velocities. To eliminate, as much as possible, the effect of vertical load, four distribution diagrams were made, one for each increment of applied vertical load. These are presented in Figs. 15 through 18. The four curves drawn through the distributions were determined in order best to satisfy two conditions: first, they were to represent the trends in the four groups of data with due regard to the quality rating of each point, and second, they also were expected to have the same general shape, thus comprising a family of curves when grouped together as in Fig. 19. Because of the dispersion present in the coefficient of friction vs. velocity distributions, in the attempt to satisfy the above two conditions, a certain amount of averaging was required, resulting in curves which were not always the best approximations to the data points. Normally, the deviations of the general trends from the best approximations were not large. However, it may be noted in Fig. 15 that the coefficients obtained at the higher velocities during this series are, in general, 15 to 20 percent lower than the curve. Since the reliability of most of these points had previously been assigned a poor rating, the compromise was not considered excessive. This portion of the curve is presented with a broken line, however, to illustrate the larger-than-average deviation. The dashed lines above and below the trend curves, in Figs. 15 to 18, enclose the ± 15 percent bands and thus offer a gauge as to the accuracy of the data.

2.4 Coefficient of Friction vs. Vertical Load

The composite of the four curves, Fig. 19 shows some variation in the coefficient of friction with applied vertical load; however, it must be remembered that, for each increment of applied load, the tire pressure was also varied in an attempt to maintain a constant rolling radius of the tire. Therefore, any deductions regarding a functional relationship between the coefficient and the applied vertical load which may be obtained from a consideration of Fig. 19 would be valid only under the condition of maintaining a constant rolling radius. A possible explanation for not observing a definite relationship between the coefficient of friction and the instantaneous vertical loading is presented in par. 3.5.

Fig. 15 Coefficient of Friction vs. Velocity Distribution Diagram Showing Trend and ± 15 Percent Band Performed with 5000 Pound Applied Vertical Load, 103 psi Tire Pressure, and 32% Tire Deflection

Fig. 16 Coefficient of Friction vs. Velocity Distribution Diagram Showing Trend and ± 15 Percent Band
Performed with 6000 Pound Applied Vertical Load, 124 psi Tire Pressure, and 32% Tire Deflection

Fig. 17 Coefficient of Friction vs. Velocity Distribution Diagram Showing Trend and ± 15 Percent Band Performed with 7000 Pound Applied Vertical Load, 145 psi Tire Pressure, and 32% Tire Deflection
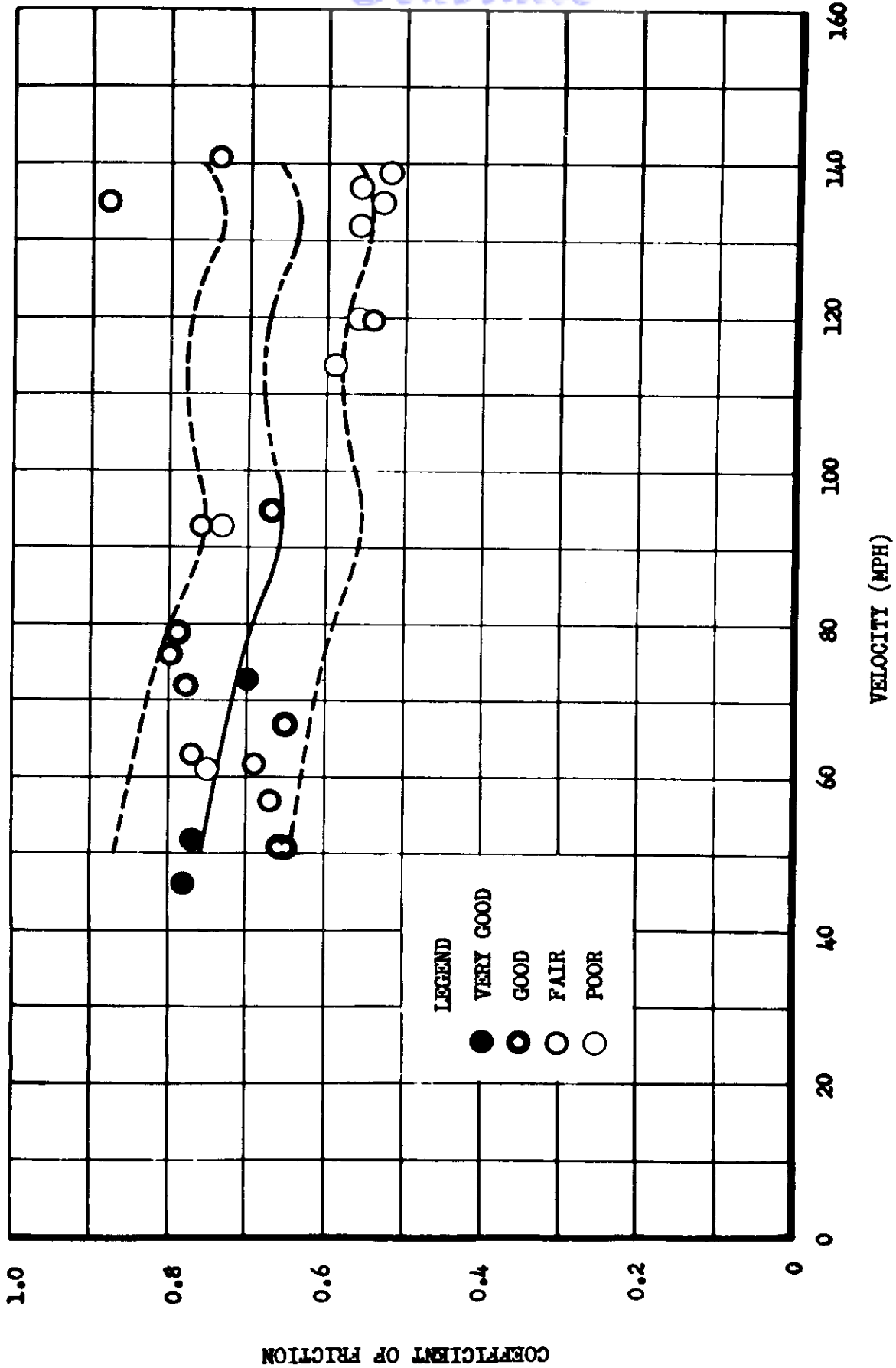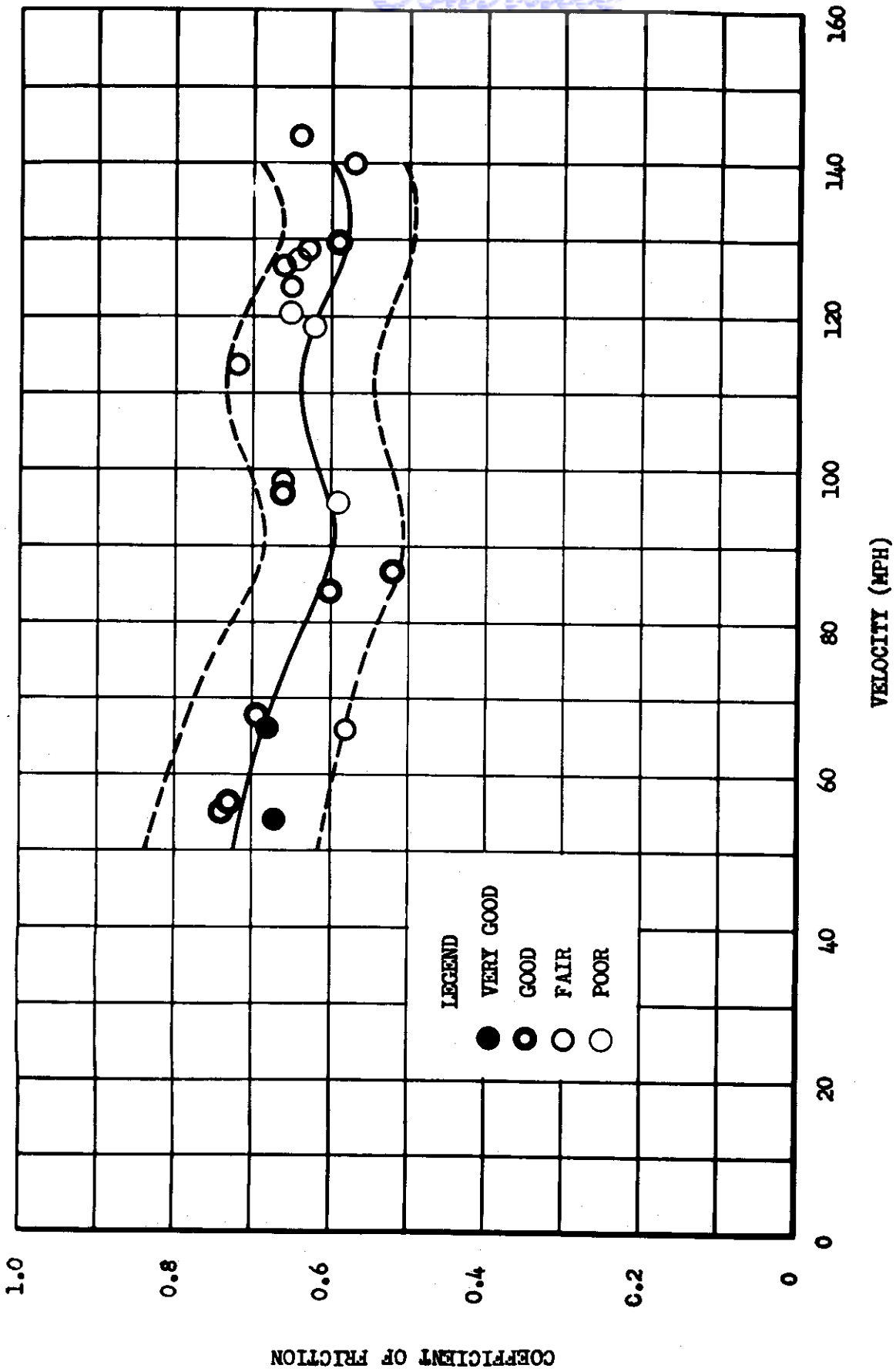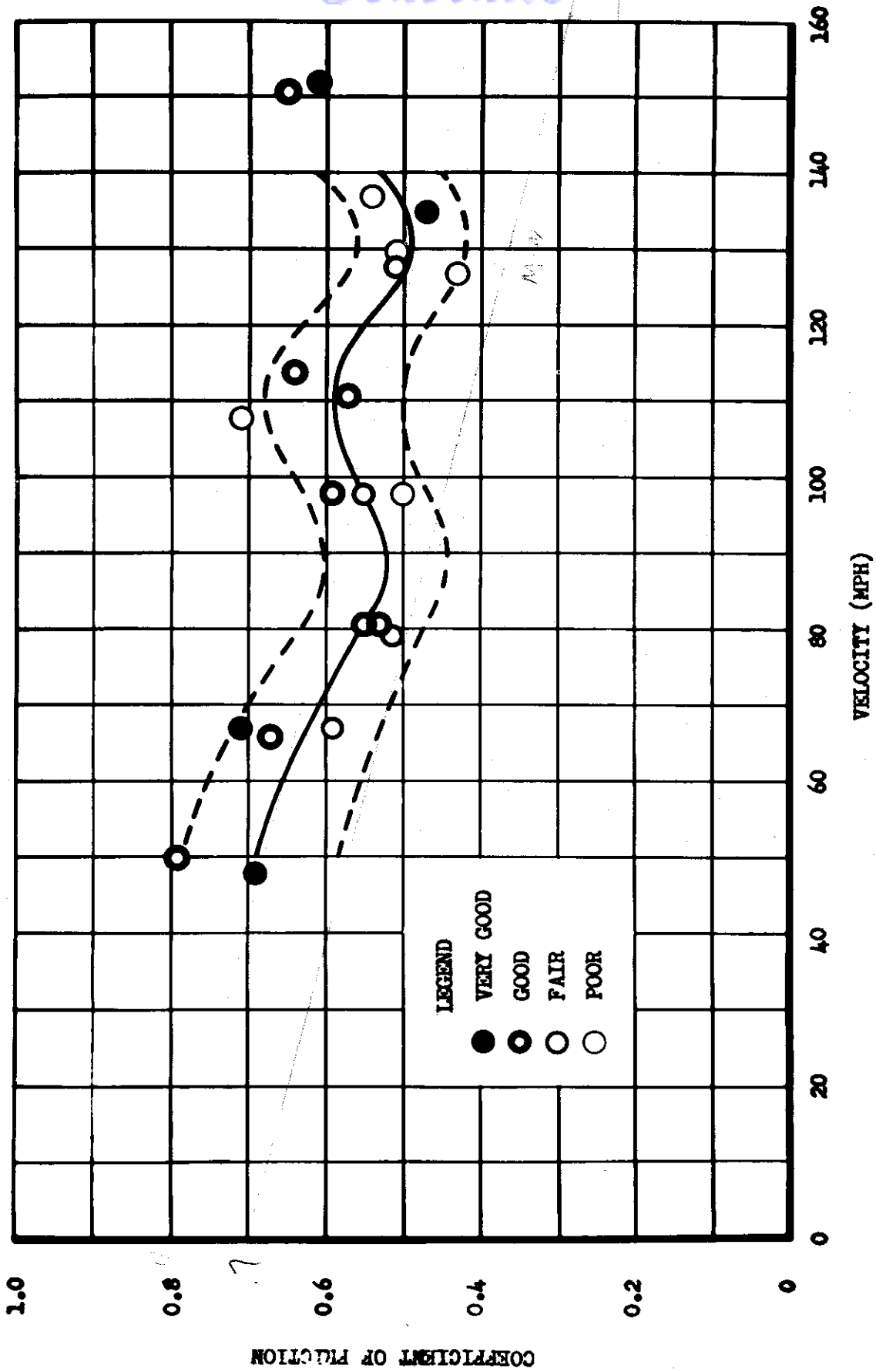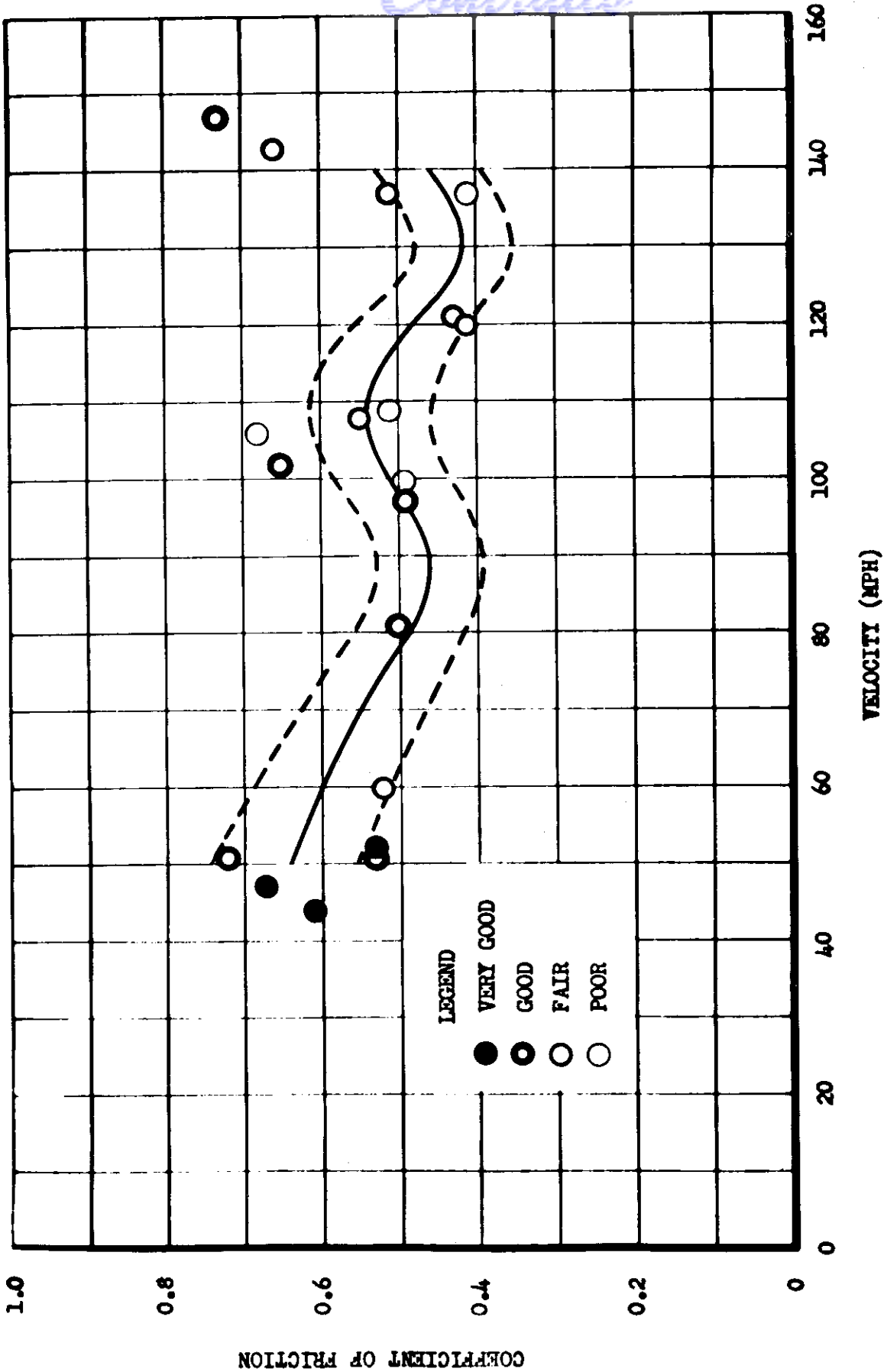
Fig. 18 Coefficient of Friction vs. Velocity Distribution Diagram Showing Trend and ± 15 Percent Band Performed with 8000 Pound Applied Vertical Load, 165 psi Tire Pressure, and 32% Tire Deflection
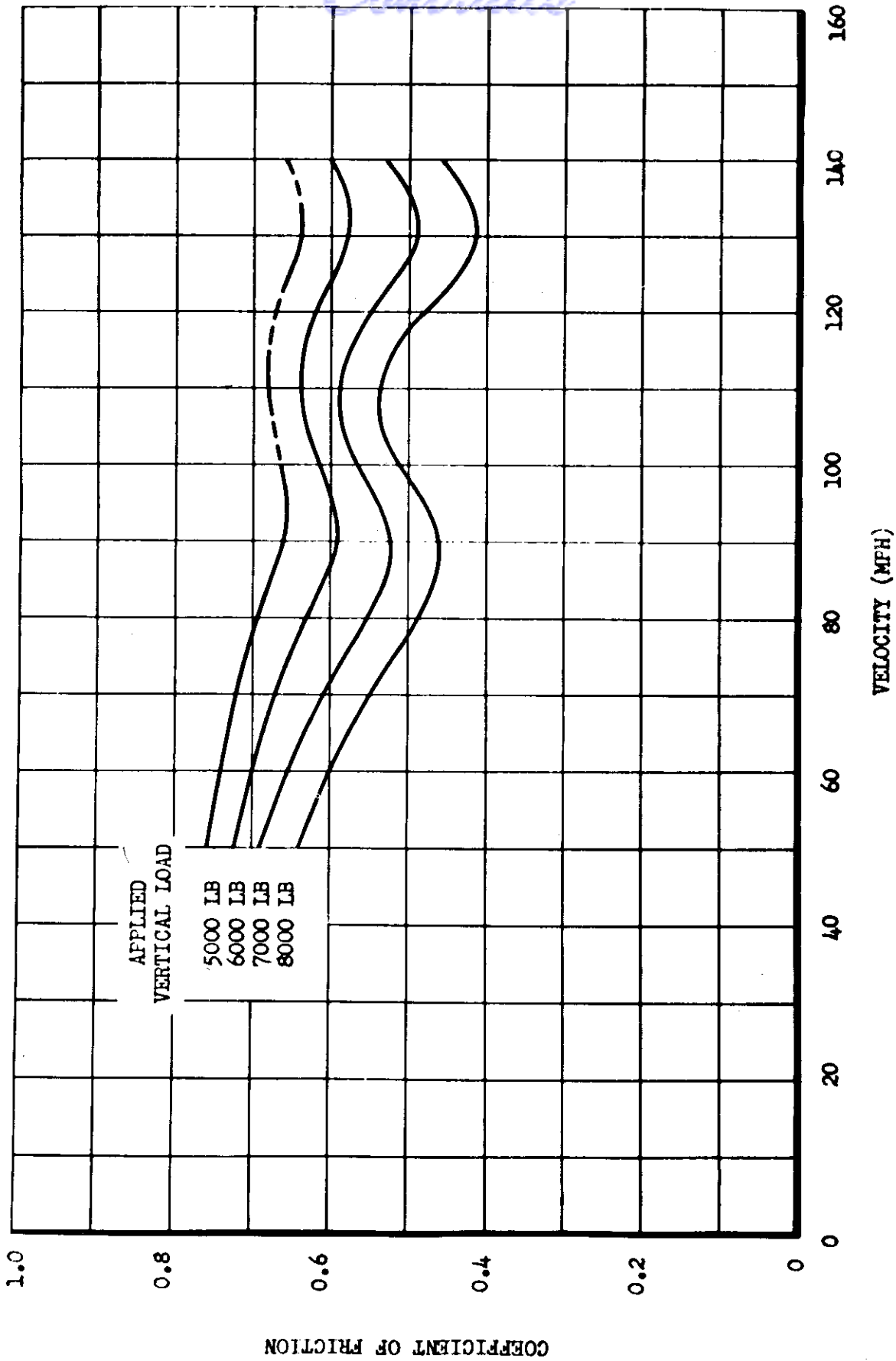
Fig. 19 Coefficient of Friction vs. Velocity Curves for Various Applied Vertical Load Maintaining 32% Tire Deflection

DISCUSSION

3.1 General

In view of the numerous factors which can effect the coefficient of
friction and its determination and of the accuracy with which the test results
were obtained, the project may well be regarded as successful. Despite
the fairly high degree of scatter present on some of the coefficient of friction
time history curves, it is believed that the individual maximum values are
within 10 percent of their true values. The figure of 10 percent was es-
tablished as the probable maximum error resulting from the various measure-
ments, corrections, and computations involved. Regarding the coefficient
of friction vs. velocity curves, the best indication of their accuracy is the
fact that the 15 percent bands shown with the curves in Figs. 15 through 18
contain 84 percent of all data points up to 140 mph. Of those points not
within the band, over 60 percent had previously been assigned quality ratings
of fair or poor.

3.2 Uncontrollable Parameters

In the Introduction to this report were listed several controllable
factors which were believed to be influential in establishing the maximum
coefficient of friction attainable during any one skid; in addition to these,
there are other parameters over which control is practically impossible,
which may similarly have affected the values obtained. Such things as wear
suffered by the runway, as well as the presence of dust and sand and even
rubber deposits from previous landings can, conceivably, affect the coefficient
of friction to such an extent that the dispersion of points on the coefficient vs.
velocity diagrams could not reasonably be attributed entirely to errors of
measurement. As for the wear of the runway, since some sections are, of
necessity, used more frequently than others, it is almost inconceivable that
identical conditions of surface roughness could exist for its entire length.
The presence of dust and sand on the runway would most certainly reduce the
maximum attainable coefficient in that the particles would tend to act as small
ball-bearings between the skidding surfaces. Also, rubber deposits from
previous landings or brakings could affect the values obtained for the coefficient
of friction since ths skidding surfaces would essentially be rubber on rubber.
Due to these conditions, as well as the probable existence of others, it appears
unlikely that any sequence of skids, performed under identical conditions of the
controllable parameters, would yield completely consistent results.

3.3 Reliability of Results

As a consequence of the material presented in the above paragraph, it
appears reasonable that the degree of accuracy obtained in the test results is
completely compatible with the reliability expected from any practical application
thereof. Since no absolute statement regarding exact surface conditions can
be made for any practical example, approximations must be accepted and, in
such cases, no reason is known why the reported results can not be accepted
with complete reliability.

3.4 Shape of Coefficient of Friction vs. Velocity Curves

Although no explanation can be offered at this time for the random shape of the coefficient of friction vs. velocity curves, a number of arguments present themselves which tend to substantiate their appearance as shown in Figs. 15 through 18. First, all four groups of data obtained for the various increments of applied vertical load definitely exhibit the same general trend as indicated. The analysis of the data showed that no other family of curves, similar to that in Fig. 19, would better represent the data in the sense described in par. 2.3. Secondly, from a negative standpoint, no theory is known to exist which would contradict the curves as presented. Finally, although the magnitude of the coefficients differed widely, the same general shape of the curves was obtained during a previous skid test program and was presented in the Memorandum Report referenced in the Introduction of this report.

3.5 Coefficient of Friction vs. Vertical Load

Apart from the variation in the coefficient with the applied vertical load as indicated in Fig. 19, no correlation between the two was observed. However, it cannot be assumed that a relationship does not exist. Actually, the rapid variations in the vertical load during the skids, as may be noted in Figs. 9 through 12, caused such adverse results that any indication of correlation may have been obscured. The effect of the varying load may be best explained as follows: ideally, the drag load experienced by the tire and strut should, at all times, be proportional to the existing vertical load; however, a certain response time due to the flexibility of the tire, was required for any variation in vertical load to be reflected in the drag measurements. This response time was most certainly greater than the time duration of some of the measured, vertical load variations, and consequently, the drag load could not maintain its proper magnitude. For such situations, the computed coefficients would not be accurate, the errors involved appearing as scatter on the coefficient of friction time history curves. In the event, however, that the vertical load was varying rapidly through the interval in which the coefficient of friction was attaining its maximum value, that maximum value would be applicable only for the average or effective vertical load during the interval. In an attempt then to analyze the data for correlation between the coefficient of friction and the vertical load, a determination of the effective loadings was required. In the absence of an analytical method for such a computation, the vertical load time histories were used for the estimation of the effective values. The results thus obtained are presented as Effective Vertical Loads in the Table of Appendix IV. The inaccuracies inherent in such a process can admittedly be quite large, and the absence of correlation between the parameters in question is believed to be due largely to these inaccuracies and to the conditions discussed in par. 3.2.

3.6 Tire Vibration During a Particular Partial Skid

The high speed photography of one, and only one, of the skid attempts revealed a series of tire vibrations in the neighborhood of the ground contact area. The vibrations appeared to be of two types. The first, and most violent, occurred at about 30 degrees of arc behind the contact area when the bead of the tire vibrated in a radial direction with an amplitude sufficient to cause an apparent separation between the bead and wheel rim of approximately 1/2 inch. The second type of vibration was wave-like in nature,
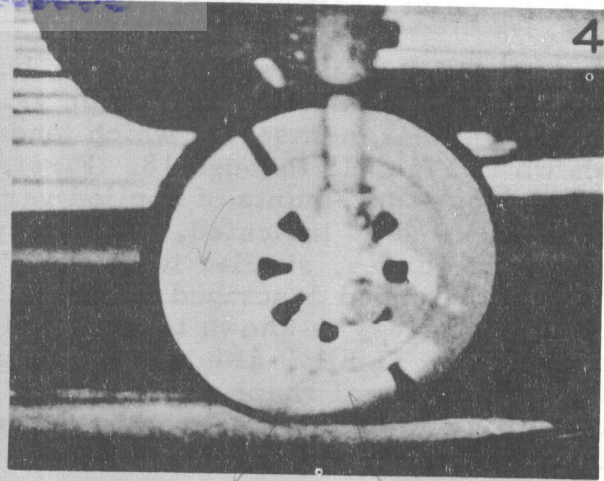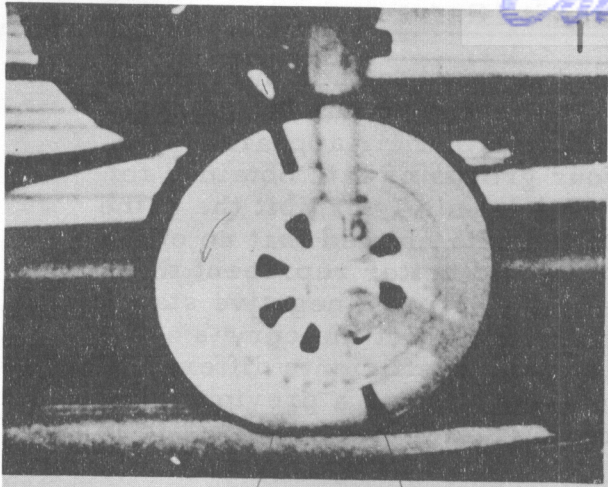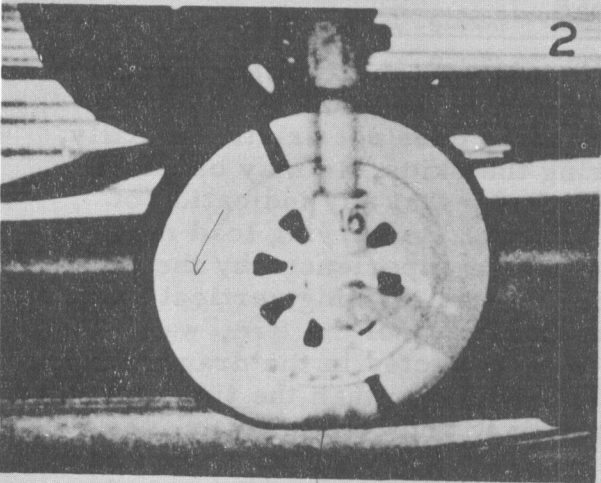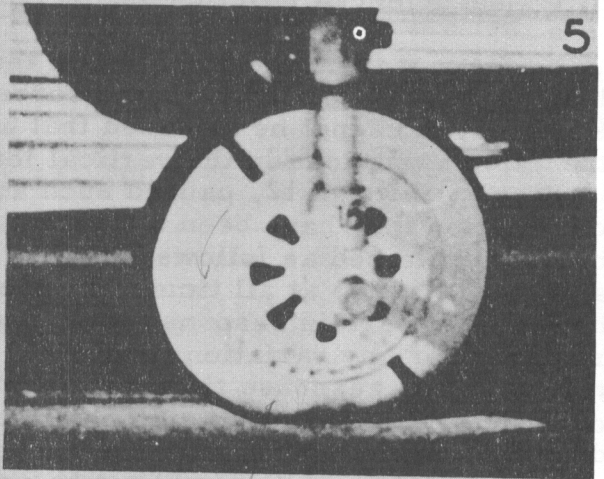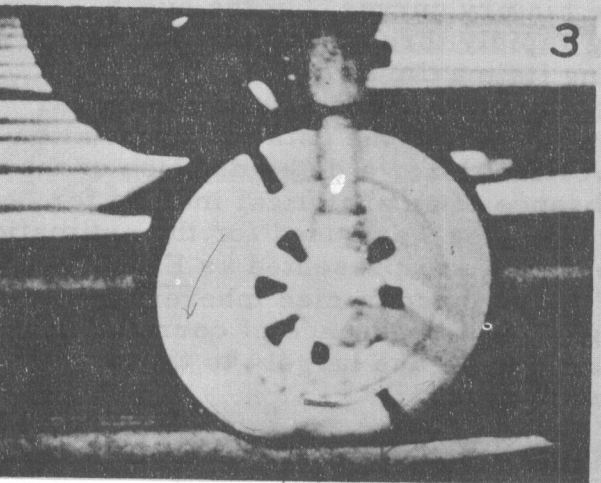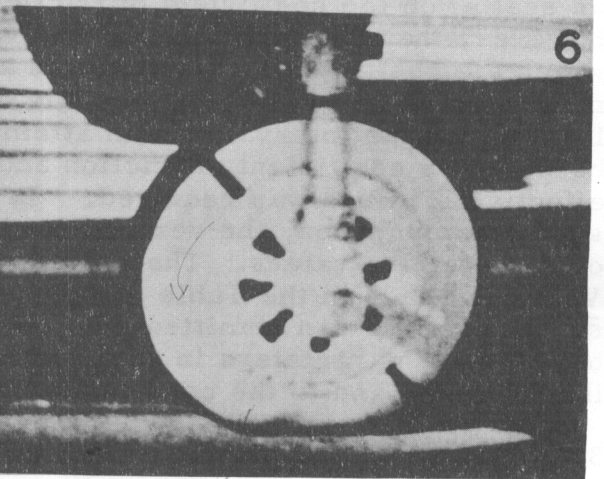
Fig. 20 Sequence of Six Frames Taken from High Speed Photographs During
Attempted Skid. Note Ripple on Side of Tire Progressing Forward
(Left). Camera Speed 1260 Frames Per Second

appearing on the side of the tire casing and traveling forward from the first vibration, past the ground contact area, to a point about 45 degrees of arc in front of the contact area. The progression of the wave-form is shown in Fig. 20 in a sequence of six frames from the high speed camera. In the pictures the wheel is rolling from right to left. The first frame shows a ripple just forward of the contact area and another just starting in the vicinity of the black radial stripe on the tire. In the second frame the new wave has traveled forward to a point just below the axle and, in the next two frames, is seen to continue its forward motion until, in the fifth frame, it is no longer visible. In the meantime another wave-form has started, in the fourth frame, and is still visible on the sixth. The camera speed during this sequence of exposures was approximately 1260 frames per second or one frame each 0.79 millisecond. Since any one ripple existed for at most five frames, its duration was approximately 3.95 millisecond; also, with a new wave starting each third frame, the period of vibration would be 2.37 millisecond. The radial vibration described first was not clearly visible on any single frame; however, when properly viewed on a screen, it appeared quite violent. The entire sequence of film is obtainable for study from the Mechanical Branch of the Aircraft Laboratory, Wright Air Development Center, Dayton, Ohio.

For the possible future determination of the causes of such vibrations, the details of the skid are as follows. The ground speed of the vehicle was 120 mph, and sufficient braking occurred to cause a relative velocity between the tire and runway of 59 mph at the time the pictures of Fig. 20 were taken. The partial skid lasted approximately 1.4 seconds with the vibrations occurring during two definite intervals. In an attempt to explain the vibrations, various parameters were investigated. The only factor which appeared to be related to the vibration was the relative velocity. Fig. 21 shows a time history of the relative velocity and also indicates the periods during which the vibration
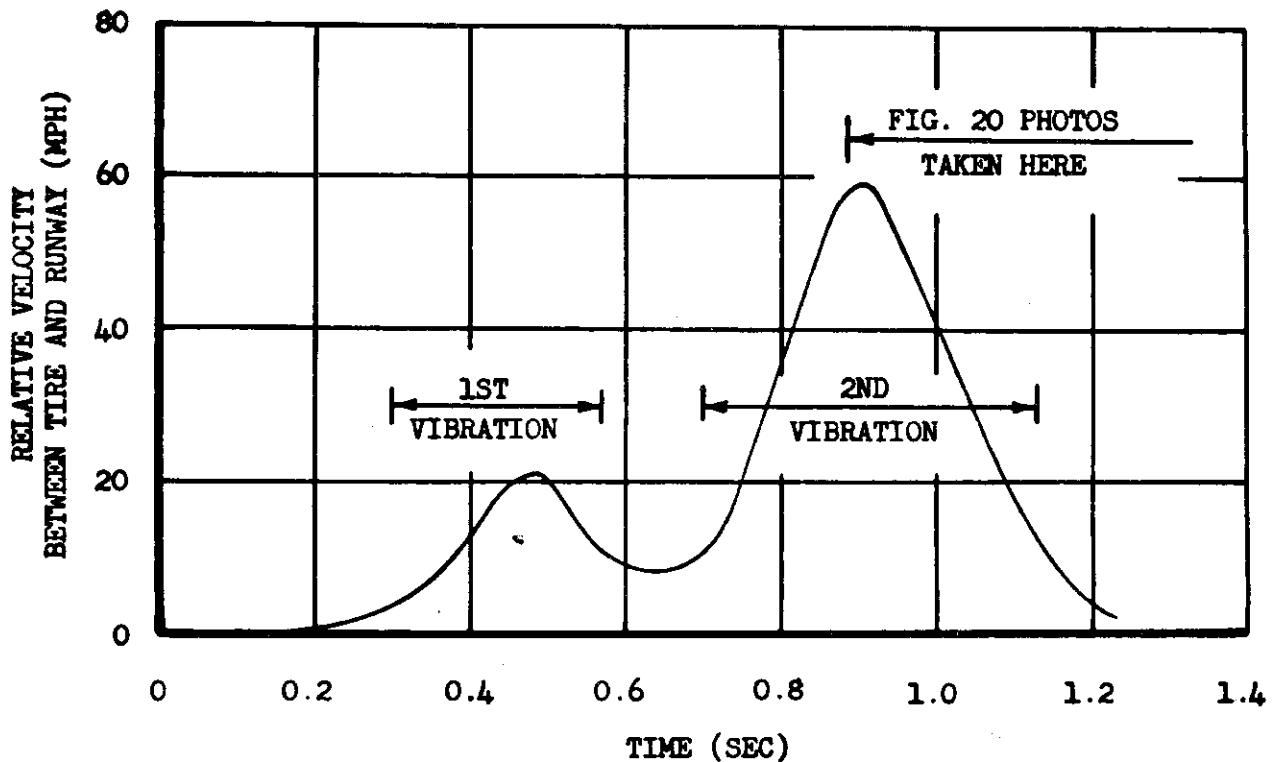
Fig. 21 Relative Velocity vs. Time Curve During Partial Skid Resulting in Violent Tire Vibration

occurred. Decreased braking action at about 0.6 second allowed a more free rotation of the wheel and resulted in a temporary interruption of the vibrations. It should also be pointed out that the vibration, besides appearing only at the higher values of relative velocity, seemed to increase in violence when the peak relative velocities were attained. The vertical load was approximately 4200 pounds at 0.9 second but varied throughout the skid between 3200 and 6700 pounds. The tire pressure was 105 psi before the skid and 110 psi afterward.

CONCLUSIONS AND RECOMMENDATIONS

4.1 Conclusions

It is concluded that:

1) The method used on this project for obtaining skid test data is adequate and reliable.

2) The results presented in this report are sufficiently accurate for general applications.

3) The maximum coefficient of friction attainable during a skid depends partially upon the velocity, nominal vertical load, and tire pressure existing during the skid.

4) No accurate relationship between the coefficient of friction and instantaneous vertical load can be derived from the test data obtained during this project.

4.2 Recommendations

It is recommended that:

1) Values currently used for the maximum attainable coefficient of friction be revised so as to correspond to the data herein reported.

2) Additional skid tests be performed in an attempt to evaluate the relationship between the coefficient of friction and the instantaneous vertical load.

3) Additional skid tests be performed on other types of runways to obtain data similar to that presented in this report.

4) A theoretical study be made of the variation in the coefficient of friction with skid velocity in an attempt to explain the apparent random relationship between the two.

5) In any future skid tests, some means should be devised whereby the vertical load can be held more constant during a skid.

1.1 General

The instrumentation equipment installed on the vehicle included sensing elements capable of producing electrical output signals with currents proportional to the phenomena being measured and an oscillograph and bridge balancing unit for the continuous recording of these output signals.

1.2 Recording Equipment

The oscillograph used was a Consolidated Engineering Company, Type 5-114-P-3, 18 Channel recording oscillograph operated on 26 v.d.c. power supplied by standard aircraft batteries. The bridge balancing unit was a Consolidated Type 8-108, 8 channel bridge balance operated at 12 v.d.c., also supplied by aircraft batteries.

1.3 Bridge Channels

Of the eighteen recording channels available on the oscillograph, only twelve were used. Of these, eight were so-called bridge channels employing essentially the standard Wheatstone bridge wiring configuration shown in Fig. 22, where the oscillograph is represented simply by a galvanometer. The diagram has been over-simplified in that the bridge balance has been omitted entirely. It suffices to say that the purpose of the unit is to provide: (1) a means of eliminating any small unbalance in the bridge due to slight differences in the resistances of the various arms, (2) a system for introducing a known unbalanced condition into the bridge for calibration and data reduction purposes explained in Appendix III, and (3) a means of attenuating the bridge outputs, if necessary, and simultaneously maintaining proper damping conditions for the oscillograph galvanometers.
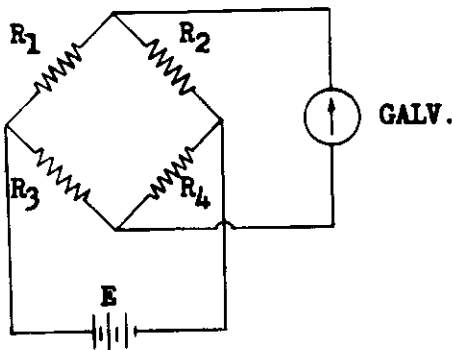
Fig. 22 Basic Wiring Configuration for all Bridge Channels

1.3.1 Load Measuring Channels

The sensing elements used for measuring the vertical, drag, and side loads were Baldwin-Lima-Hamilton, Type U-1 load cells, the capacities of which are given in Table 1. The cells were sensitive to both compression and tension loads and were temperature compensated and hermetically sealed for protection against effects caused by variations in temperature and humidity. Each cell was a complete bridge circuit in itself, and no additional wiring was required except through the bridge balance.

1.3.2 Pitch Angle

Since the load cells measured the forces only in directions parallel and perpendicular to the strut center line, it was necessary that corrections be

TABLE I

Summary of Measurements and Sensing Elements

MEASUREMENT	SENSING ELEMENT	CAPACITY	RESOLUTION*
Vertical Load	Load Cell	10,000 lb	23 lb
Upper Drag Load	Load Cell	10,000 lb	23 lb
Lower Drag Load	Load Cell	20,000 lb	48 lb
Upper Side Load	Load Cell	2,000 lb	13 lb
Lower Side Load	Load Cell	5,000 lb	29 lb
Strut Accelerating Force	Linear Accelerometer	±12 g	30 lb
C. G. Acceleration	Linear Accelerometer	±6 g	0.008 g
Pitch Angle	Vertical Gyro Unit	-	0.016 deg
Ground Speed	Tachometer Generator	-	0.83 mph
Wheel Speed	Contactor Device	-	-

* Amount of measured quantity per 0.01 inch of oscillograph trace deflection.

applied to the measured loads to compensate for the attitude of the vehicle as explained in Appendix III. Toward this end, a vertical gyro component and a chassis assembly of an E-6 autopilot unit was obtained to be used as the sensing element for the determination of the instantaneous pitch angle. The chassis assembly was mounted on the bomb bay platform, and the gyro unit was located on the bomb bay fixture as shown in Fig. 3. The pitch potentiometer of the gyro component which is normally used to drive the elevator control servo motor was powered by 1.5 v.d.c. from the bridge balance and was wired into the bridge circuit shown in Fig. 23. The potentiometer was mounted to the base of the unit
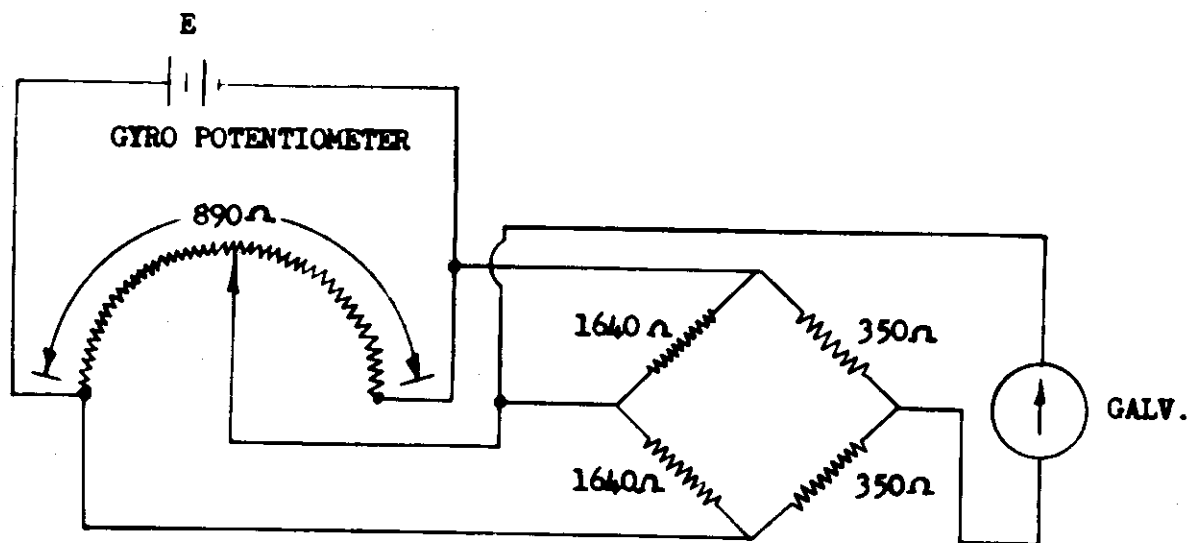
Fig. 23   Wiring Diagram for Measurement of Pitch Angle

and the wiper affixed to the rotor cage always maintaining a vertical position so that the angular deviation of the wiper from the true center position was equal to the pitch angle and the degree of unbalance caused in the bridge circuit was proportional thereto. The erection motor in the gyro is normally energized by a mercury switch which could, during periods of acceleration and deceleration, cause over-erection of the spin axis and hence had to be disconnected during the runs.

1.3.3 Acceleration Measuring Channels

Because of the inability of the load cells to measure the exact forces experienced by the tire and strut, it was necessary to install an accelerometer to determine the instantaneous accelerating forces. Also, considering the fact that any appreciable deceleration of the entire vehicle experienced during a skid would be reflected in a strut acceleration measurement, it was decided to measure not only the acceleration of the strut but also that of the vehicle at or near its center of gravity. The measurements were made utilizing Statham Model A-18 linear accelerometers with ranges of ± 12 and ± 6 g's for the strut acceleration and c.g. acceleration, respectively. Each accelerometer was a complete bridge and required additional wiring only to energize the 12 v.d.c. heater circuits to eliminate temperature effects.

1.4.1 Ground Speed

The ground speed of the vehicle was measured by calibrating and recording the output of a tachometer generator responding, thru a pulley arrangement, to the radial velocity of an auxiliary trailing wheel mounted on the right main strut. The installation, shown in Fig. 6, included an additional generator to drive a tachometer in the pilot's compartment for a determination of the ground speed during the skid tests. The wiring diagram for the ground speed channel is shown in Fig. 24.
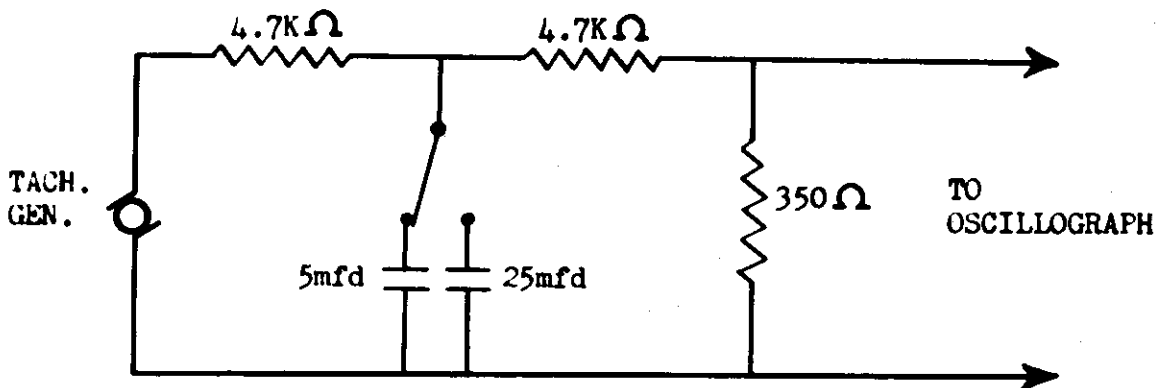
Fig. 24 Wiring Diagram for Ground Speed Measurement

1.4.2 Wheel Speed

The peripheral speed of the test wheel was determined by the contactor device shown in Fig. 7 and wired according to Fig. 25. As the wheel, and therefore the brake discs, rotated, contact was made and broken three times per revolution, and three pulses were impressed on the oscillograph galvanometer. The speed of the wheel could then be determined by noting the elasped time between pulses on the oscillograph trace as indicated by the 0.01 second timing lines on the record.

1.4.3 Photographic Coordination

In order to provide coordination between the photographic and the oscillographic data, a 100 cps pulse generator and amplifier was installed in the vehicle by the Technical Photographic Unit of WPAFB. The output signal was wired to both the oscillograph and the cameras in accordance with the block diagram shown in Fig. 26. The micro-switch indicated in the diagram was normally open; it was operated by the brake lever, and served two purposes. First, at the time the brake was applied both the oscillograph and the cameras were operating, and the first pulse, following the closing of the switch, was thus recorded by both devices and hence established the proper correspondence between the instruments. Second, by adjusting the micro-switch so that the circuit was closed at the instant the brake lever started forward, the first pulse also established the starting time of the brake application.
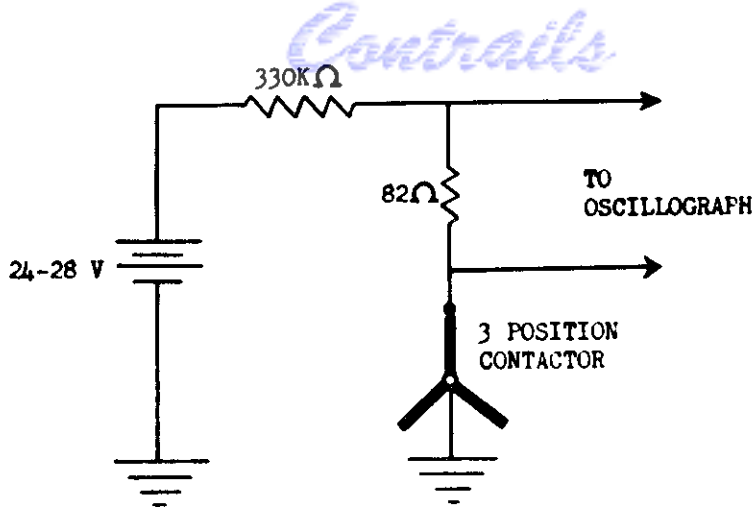
Fig. 25 Wiring Diagram for Wheel Speed Measurement

1.4.4 Bridge Voltage Monitor

The operating voltage applied to the bridge balance was monitored by impressing, on an oscillograph galvanometer, a signal proportional to the applied voltage. The signal was obtained by a voltage divider within the bridge balance. The measurement was required since a fluctuation in the bridge voltage is the only factor which affects circuit sensitivities which is not accounted for by the resistance calibration procedure described in par. 2.2 of the Appendix.
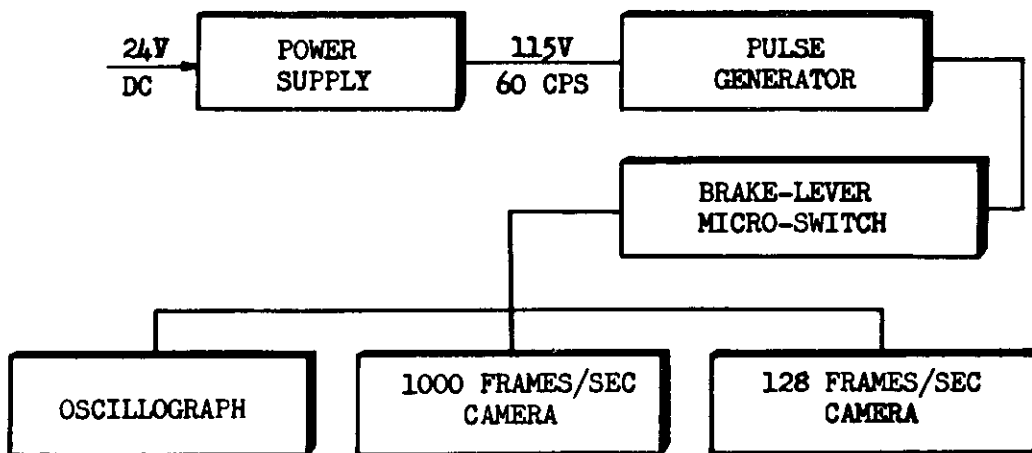
Fig. 26 Block Diagram Showing Essential Components for Photo-Oscillographic Coordination Pulses

Calibration

2.1 General

The calibration of any system, designed to measure a specific phenomenon, consists of a determination of the over-all system response to the phenomenon being measured. When this determination is accomplished by an actual measurement of the system response to known quantities of the variable, the calibration is empirical. This is the method used to calibrate each of the installations described in Appendix A, with the exception of the wheel speed measurement. However, the over-all sensitivities were subject to change due to slight variations with in the systems, usually in the electrical components, and, in order to compensate for these changes, a method known as the Resistance Calibration Procedure was used.

2.2 Resistance Calibration

The resistance calibration procedure was devised to reduce to an irrelevant status any variation in a calibration caused by a change in the sensitivity of the measuring system. This is accomplished by referring the system response, not to an absolute measure, e.g., the deviation in inches of an oscillogram trace from its balanced or zero position, but rather to the corresponding response of the system to a known and accurately controlled input or calibrate signal. This reference is made on a percentage basis whereby any given load being measured will always effect the same system response, when compared to the response of the system to the calibrate signal, regardless of minor variations in sensitivity.

In view of the instrumentation used during the project, all responses were recorded as trace deflections from predetermined zero positions, and hence the procedure used during calibration involved only the following five steps: (1) The introduction of a calibrate signal, by means of destroying the balance of the bridge by the addition of a known resistance across one of the bridge arms, (2) the determination of the trace deflection caused by the signal, (3) the application of various known loads and the measurements of their trace deflections, (4) the conversion of these deflections to their percent values of the calibrate deflections, and (5) the plotting of the data as load versus percent of calibrate deflection, generally termed percent cal. The use of the calibration curve entails only the conversion of the deflection caused by an unknown test load to its percent cal value and obtaining from the calibration curve the corresponding load.

2.3 Load Cells

2.3.1 Laboratory Calibration

All of the load cells used for the vertical, drag, and side load measurements were calibrated for their appropriate loads, either tension, compression or both, in a Riehle Testing Machine. Calibrate signals, as described in the preceeding paragraph, were applied to the system for each cell prior to the

application of any load. For each calibration the degree of unbalance intro-
duced into the system was sufficient to cause a trace deflection of approxi-
mately two inches. The loads were applied in increments of 10% of the cell
capacities up to the maximum rated loads of the cells and then decreased in
the same increments. Oscillograph records were taken for each increment,
and the trace deflections were converted into percent cal values. These
values were plotted against the applied loads to obtain calibration curves, all
of which were linear. The slopes of the curves were taken as the cal factors
in units of lbs per % Cal.

2.3.2 Vehicle Calibration

In addition to the laboratory calibrations of the load cells, each of the
vertical, side, and drag load system responses was again calibrated on the
vehicle to verify the theory behind the measurements for at least a static
condition. A special fixture was fabricated to replace the tire and wheel
during the calibrations. The fixture fitted over the axle and was bolted to the
brake flange. It was designed in such a way that the various drag and side
loads could be applied at a distance from the axle center line equal to the
rolling radius of the tire.

The vertical load calibration was accomplished by lowering the
fixture onto a steel plate supported by three load cells from a standard Cox
and Stevens Aircraft Weighing Kit. The load was applied by increasing the
hydraulic pressure against the down side of the carriage operating cylinders
on the bomb bay fixture. Loads were applied in increments of 20% of the
cell capacity up to approximately 9000 pounds. The cal factor thus obtained
was approximately 1% lower than that obtained by the laboratory calibration
and was attributed to the lower accuracy of the weighing kit load cells and
to the possibility of eccentric loading of the vertical load cell due to a deviation
of the strut center line from a true vertical position. The cal factor obtained
from the laboratory calibration was used in the reduction of the test data.

The side load calibration on the vehicle consisted of applying loads
hydraulically in both the right and left directions in increments of 200 pounds
up to 1000 pounds for each of three vertical load settings, namely 0, 4000,
and 6000 pounds. The purpose for varying the vertical load was to establish
the effect, if any, of vertical load on the side load measurements. The
results of the calibration showed some correlation between the two loads,
but in view of the purpose of measuring the side load, as explained in par. 1.1
in the body of the report, the correlation was not of sufficient magnitude to
affect the final data.

The drag load calibration on the vehicle was also conducted for various
vertical loads. Here, the effect of the vertical load was expected to be quite
appreciable. The strut, having a relatively low moment of inertia in the drag
direction, would deflect under the anticipated loads allowing a definite eccentric
loading condition in the vertical direction resulting in still more deflection.
Actually, three complete calibrations were performed before an acceptable
correction for this reaction was determined. The first calibration involved
the variation of the drag load for constant vertical loads of 0, 4000, and
6000 pounds; the second, by holding the drag load constant at 500 pound
increments from 1000 to 2500 pounds and, for each increment, varying the
vertical load from zero to 6000 pounds. During both of these attempts, the

load which was to be held constant was applied at the beginning of the cali-
bration and was altered with each change in the other variable, such that
it did remain constant. However, due either to the hysteresis of the strut
or to inaccuracies in the applied loads, the data obtained from the oscillograph
records of these two calibrations did not exhibit any reasonable trends which
were sufficient for the determination of an adequate drag load correction.
The third calibration was performed in a manner similar to the first, in that
the vertical load was set initially but allowed to vary as the drag load was
varied. The calibration was also performed for more and higher values of
vertical load. The drag load was varied from 0 to 3000 pounds for each of
the vertical loads of 3000, 4000, 5000, and 6000 pounds. The results of the
calibration indicated that the measured drag load should be decreased by
an amount equal to 1.0×10^{-5} times the product of the measured drag and
vertical loads, this being the correction, dependent upon both the loads, for
which the average difference between the applied and the corrected drag
loads was a minimum. The effect of a drag load on the measured vertical
load was negligible. The calibration data for the nominal vertical load
setting of 6000 pounds is presented in Table II together with the cor-
rected drag load and the computed differences. The value of 6000 pounds
was chosen merely because it was the most representative of the loads ex-
perienced during a test skid.

2.4 Accelerometers

In order that the acceleration forces acting on the strut might be
accounted for, it was necessary that a value of the net strut acceleration be
obtained. To accomplish this it was anticipated that the c.g. acceleration
would have to be subtracted from the measured strut acceleration. Since
the subtraction of the accelerations could only be made when the measure-
ments were in the same units, it was planned to convert both measurements
to g's, perform the subtraction, and then convert the net strut acceleration
to pounds of accelerating force. This necessitated a calibration of the
center of gravity accelerometer in g's vs. accelerometer output and two
calibrations for the strut accelerometer, namely, g's vs. output and
accelerating force vs. g's. The calibrations of both accelerometers for g's
vs. output were performed in the laboratory. The calibration of the strut
accelerometer for force vs. g's was obtained by first calibrating for
accelerating force vs. output and then converting the output of the accelerometer
to g's by means of the previous laboratory calibration. The eventual use of
the two acceleration measurements is explained in par. 3.3.3 of the Appendix.
A description of the calibration procedures is given in the following sections.

2.4.1 Laboratory Calibration

Both accelerometers were calibrated in the laboratory to determine
their outputs in units of g's per percent cal trace deflection on a shake-
table with a fixed amplitude of vibration. To obtain the various values of
acceleration, the frequency of vibration was altered. Both calibrations
were carried out by taking oscillograph records at approximately 10%
intervals up to the accelerometer capacities. The percent cal deflections
were plotted for both positive and negative accelerations, and both plots
revealed very good linearity.

TABLE II

Drag Load Calibration Data for Initial Vertical Load of 6000 lb Showing Effect of Drag Load

Correction for Strut Bending

Applied Drag Load D_A	Measured Drag Load D_M	Measured Vertical Load V_M	Correction $D_M \cdot V_M \cdot 10^{-5}$ C	Corrected Drag Load $D_C = D_M - C$	Difference $D_C - D_A$
0	0	5903	0	0	0
500	563	5583	31	532	32
1000	1016	5370	55	971	-29
1500	1567	5156	81	1486	-14
2000	2118	5085	108	2010	10
2500	2599	4872	127	2472	-28
3000	3122	4623	144	2978	-22
2470	2594	4872	126	2468	-2
2020	1646	5263	87	1559	39
1000	1090	5334	58	1032	32
510	545	5512	30	515	5
0	0	5618	0	0	0

NOTE.—All values in pounds

2.4.2 Vehicle Calibration

The calibration of the strut accelerometer for output vs. accelerating force was performed on the vehicle with all equipment in place and operating. Accelerating forces were applied hydraulically in a drag direction. For the purpose of converting the applied force into accelerating force, a bomb release mechanism was included in the cable arrangement to allow a means of releasing the load instantaneously. Forces were applied and released in 100 pound increments from 100 to 1000 pounds. The plotted values of output in percent cal vs. applied force showed fair linearity, the deviation being attributed to inconsistent damping of the structure.

During the actual skidding process two strut accelerometers were damaged during tire blow-outs, and the above calibration was repeated for each new accelerometer installed.

2.5 Pitch Angle

Since the autopilot used as the sensing element in the pitch angle measurement was a self-contained unit, the calibration thereof was not required to be performed on the vehicle. It was only necessary to determine the output of the system as a function of the angle of pitch, and this was more accurately accomplished within the laboratory where the angle could be adjusted with greater precision. The calibration was carried out for one-half degree increments from a nosedown attitude of eight degrees to a noseup attitude of eight degrees. This range of angles far exceeded the pitch angles expected during actual tests but enabled the calibration curve to be drawn with more accuracy than would have been possible over a smaller range. After the calibration it was required only to mount the gyro unit in a level position on the bomb bay fixture carriage.

2.6 Ground Speed

The calibration of the ground speed installation consisted of rotating the auxiliary wheel and recording oscillographically the generator output at various speeds. Ground speeds at 25 mph intervals up to 150 mph were converted to their corresponding rpm values, and the wheel was rotated at these speeds for calibration. Wheel rotation was accomplished by the use of a motor driven cylinder equipped with a variable speed drive; the cylinder was placed against the wheel thus driving it through friction. Measurements of wheel rpm were made using a General Radio Model 631-B Strobotac.

2.7 Wheel Speed

Since the determination of the wheel speed during a partial skid involved only the determination of the time required for a series of three pulses on the oscillogram trace, no calibration was required. A functional check was performed, however, to establish the reliability of the device at the speeds expected to be attained. For this purpose, the motor-driven unit described in the previous paragraph was used.

2.8 Bridge Voltage Monitor

The response of the oscillograph galvanometer to a variation in bridge voltage was obtained by varying the voltage applied to the bridge balance from 3 to 12 volts in 1 volt increments and plotting the applied voltage against the resulting trace deflection.

DATA REDUCTION

3.1 General

In this section is included all of the various steps from the measurements of the oscillogram trace deflections to the determination of the final data required for the attainment of the test objective. Even though many of these steps were performed simultaneously by IBM computing equipment, they will be presented here as individual operations.

Just prior to each run of three skids, a procedure was followed during which oscillograph records were taken to determine the zero (no load) positions of all traces. Also, in order to establish the sensitivities of the various channels for each run, cal step records were taken in which the same unbalance used during the calibration procedure was introduced into each channel. The resulting deflection of each trace, caused by the unbalance and called the cal step was then taken as 100% for the purpose of comparing the trace deflections occurring during a skid.

3.2 Determination of Loads

The individual quantities being measured were determined, in general, at each 0.01 second interval during the partial skids just prior to the locking of the test wheel. For each channel, a measurement was made of the trace position relative to a static reference trace. From this value was subtracted the zero position of the trace, and the difference was evaluated as a percentage of the cal step and termed the percent cal deflection. The products of the percent cal deflections and the proper cal factors yielded the existing values of all quantities being measured for each 0.01 second. The uncorrected drag and the side loads were determined by taking the difference between the values indicated by the lower and upper drag and side load cells.

3.3 Corrections

The corrections to which the measured drag and vertical loads were subjected are presented in the following paragraphs in the order in which the corrections were applied.

3.3.1 Drag Load Correction for Strut Bending

Since the uncorrected drag load, as measured by the load cell responses, was primarily a measure of the degree of bending of the strut, the correction for the effect of strut bending was applied first. As explained in par. 2.3.2 of the Appendix, the correction amounted only to subtracting from the measured drag load an amount equal to 1.0×10^{-5} times the product of the measured drag and vertical loads.

3.3.2 Corrections for Pitch Angle

The uncorrected vertical and drag loads as measured by the load cells were only apparent values in that they were measured in directions parallel

and perpendicular to the strut center-line, which deviated from the true vertical and horizontal directions by the measured pitch angle. The true forces were determined by combining the vertical and horizontal components as follows:

$$V = V'Cos\,\alpha - D'Sin\,\alpha ,$$
$$D = V'Sin\,\alpha + D'Cos\,\alpha ,$$

where the primed values were the measured loads and the pitch angle α was positive for nose-up attitudes. The above relations are portrayed vectorially in Fig. 27.

D' = Measured Drag Load
V' = Measured Vertical Load

$V = V'Cos\,\alpha - D'Sin\,\alpha$
$D = V'Sin\,\alpha + D'Cos\,\alpha$
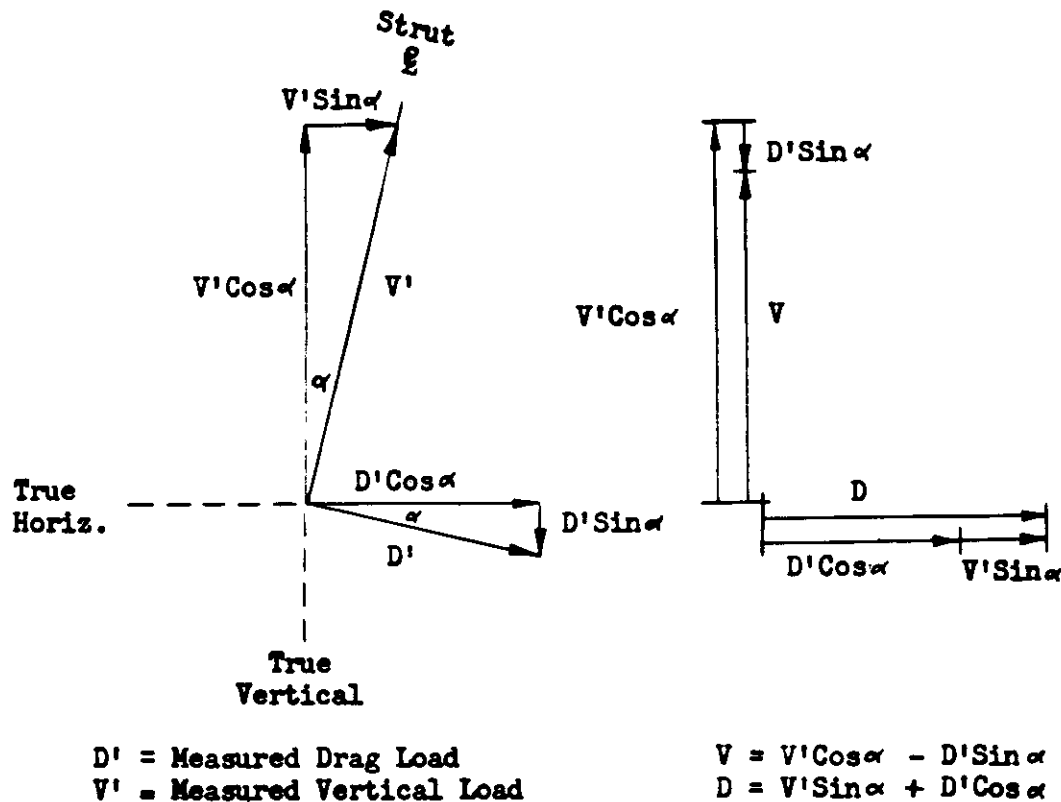
Fig. 27 Vectorial Representation of Pitch Angle Correction

3.3.3 Correction for Strut Acceleration

The planned procedure for applying a correction to the drag load to account for the strut accelerating forces was discarded early in the data reduction phase because of the extremely small c.g. accelerations relative to those of the strut. Actually, the strut acceleration trace deflections were converted immediately into pounds of accelerating force, and thus the correction simply amounted to an algebraic addition of this quantity and the drag load resulting from the pitch angle correction. The theory behind the correction is presented in Fig. 28 wherein a hypothetical instantaneous loading of 1500 pounds is applied at zero time. The measured drag load and the accelerating forces would then oscillate about the proper values such that the sum of the two forces would always equal the applied 1500 pounds. Fig. 29 shows the

measured drag load (after the corrections for strut bending and pitch angle), the accelerating force, and the corrected drag load for a particular interval during skid 6080-2. The effectiveness of the correction is apparent by the relative smoothness of the drag load curve after the application at the correction.

3.3.4 Computation of Coefficient of Friction

The original planning for the program included the combining of the side and drag loads vectorially to obtain a resultant horizontal force. The quotient of this resultant and the vertical load was then to be taken as the coefficient of friction. However, after determining the side loads experienced during the first few skids, it was felt that this load would never exceed 500 pounds. Assuming this value, the resultant horizontal force was calculated to be less than 50 pounds greater than the drag load alone. Consequently, the original planning was discarded and the coefficient of friction values were obtained by computing the quotient of the corrected drag and vertical loads.

3.4 Plotting

Time-history curves of the coefficient of friction were plotted for each skid. A smooth curve was drawn through the points and the peaks of these curves were taken as the maximum attainable coefficients for the existing values of velocity and vertical loading.
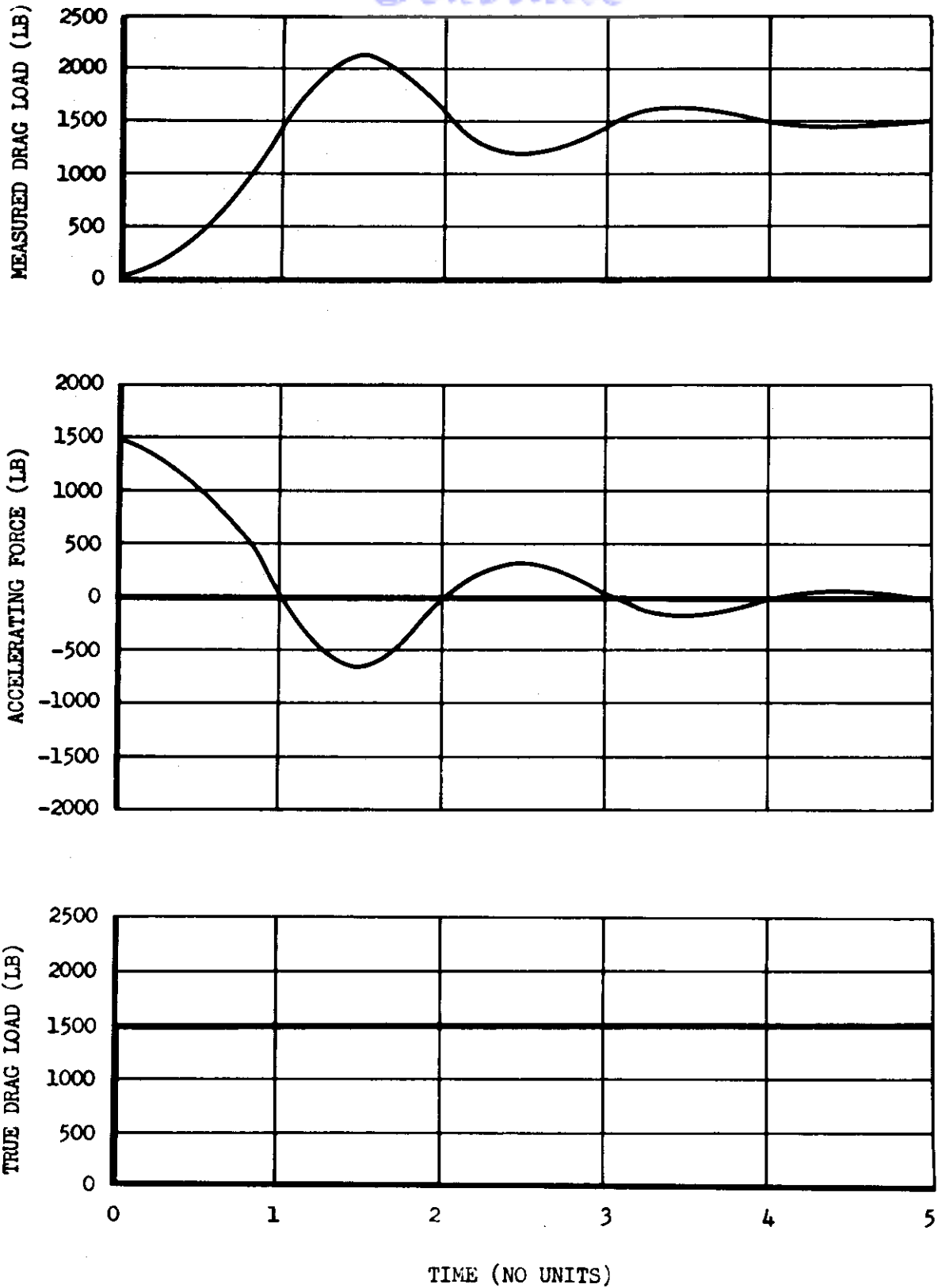
Fig. 28 Hypothetical Example Showing Theory of Drag Load Correction for
Strut Acceleration. Note that the Sum of the Measured Drag Load and the
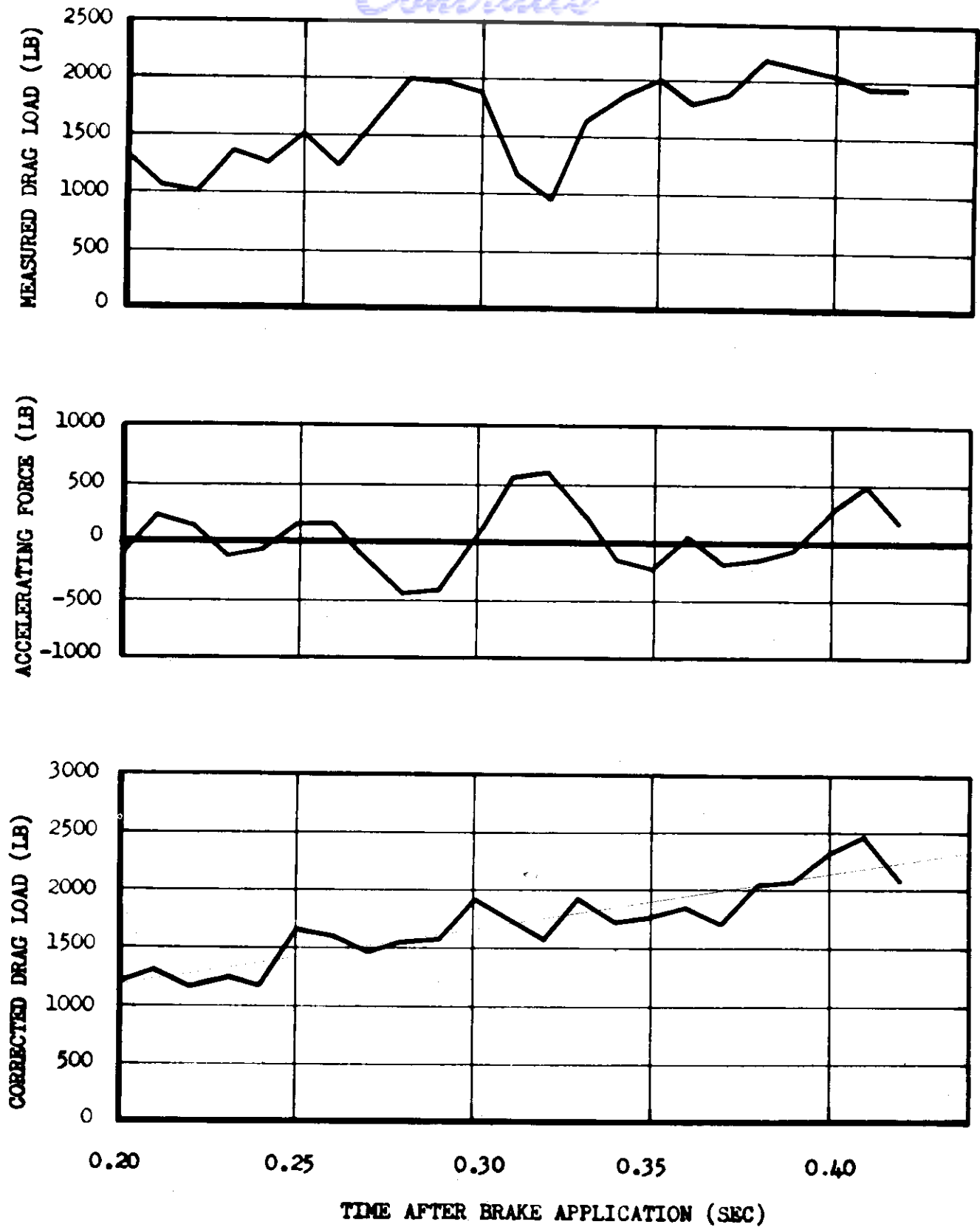Accelerating Force Always Equals the Applied Drag Load of 1500 lb.

Fig. 29 Curves of Skid 6080-2 Showing Effectiveness of Drag Load Correction for Strut Acceleration. Note Smoothing of Drag Load Curve Resulting from Correction.

APPENDIX IV

SUMMARY OF DATA IN TABULAR FORM

TABLE III

Summary of Final Data Regarding Individual Skids

SKID[1] NO.	MAXIMUM COEFFICIENT OF FRICTION	SKID[2] VELOCITY (MPH)	RELATIVE[3] VELOCITY (FPS)	EFFECTIVE[4] VERTICAL LOAD (LB)	QUALITY[5] RATING	LENGTH OF PARTIAL SKID (SEC)
5050-1	0.78	46	19	4700	V	0.76
5050-2	0.77	52	21	3950	V	0.35
5050-3	0.65	51	16	4600	G	0.35
5050-4	0.66	51	19	5100	G	0.41
5065-1	0.79	79	30	3600	G	0.92
5065-2	0.80	76	37	3950	G	0.53
5065-3	0.78	72	31	3550	G	0.30
5065-4	0.77	63	30	4000	F	0.55
5065-5	0.75	61	24	4400	P	0.60
5065-6	0.67	57	19	5100	F	0.67
5080-1	0.70	73	22	3900	V	0.33
5080-2	0.65	67	13	4600	G	0.49
5080-3	0.69	62	12	4950	F	0.48
5095-1	0.67	95	37	3700	G	0.71
5095-2	0.76	93	30	4100	F	0.49
5095-3	0.73	93	29	4300	P	0.54
5110-1	0.59	114	80	3700	P	0.73
5125-1	0.54	120	104	3800	F	0.60
5125-2	0.56	120	61	3950	P	0.38
5140-1	0.88	135	91	3500	F	0.29
5140-2	0.53	135	91	4300	P	0.29
5140-3	0.52	139	64	7000	P	0.62
5140-4	0.56	137	49	5450	P	0.49
5140-5	0.56	132	81	3850	P	0.40
5150-1	0.74	141	68	2800	F	0.31
6050-1	0.74	55	23	4300	G	0.71
6050-2	0.73	56	21	5200	G	0.84
6050-3	0.67	54	14	6300	V	0.62
6065-1	0.69	67	14	5500	G	0.73
6065-2	0.68	66	28	4100	V	0.37
6065-3	0.58	66	19	5700	F	0.37
6080-1	0.60	84	55	4500	G	0.62
6080-2	0.52	87	17	7400	G	0.78
6095-1	0.66	97	28	4600	G	0.80
6095-2	0.66	98	37	5000	F	0.42
6095-3	0.59	96	38	5300	P	0.55
6110-1	0.72	114	30	4100	F	0.81
6110-2	0.62	119	42	4500	P	0.54
6110-3	0.65	121	78	4000	P	0.73
6125-1	0.65	124	28	4800	F	0.75
6125-2	0.66	127	48	5600	F	0.76
6125-3	0.64	128	98	3950	P	0.26
6140-1	0.59	130	92	4400	G	0.51
6140-2	0.63	129	60	3800	F	0.40
6150-1	0.64	144	30	4700	F	0.53
6150-2	0.57	140	51	4250	F	0.32

TABLE III (CONT.)

SKID[1] NO.	MAXIMUM COEFFICIENT OF FRICTION	SKID[2] VELOCITY (MPH)	RELATIVE[3] VELOCITY (FPS)	EFFECTIVE[4] VERTICAL LOAD (LB)	QUALITY[5] RATING	LENGTH OF PARTIAL SKID (SEC)
7050-1	0.79	50	28	6200	G	0.98
7050-2	0.69	48	16	4350	V	0.83
7065-1	0.67	66	30	4250	G	0.80
7065-2	0.71	67	27	4600	V	0.72
7065-3	0.59	67	24	4800	F	0.81
7080-1	0.53	81	33	5900	G	0.79
7080-2	0.55	81	27	6400	G	0.61
7080-3	0.52	80	80	6300	F	0.54
7095-1	0.59	98	24	5400	G	0.83
7095-2	0.50	98	26	5000	P	0.68
7095-3	0.55	98	24	6500	F	0.46
7110-1	0.64	114	52	5300	G	0.95
7110-2	0.57	111	72	5150	G	0.85
7110-3	0.71	108	75	4350	P	1.01
7125-1	0.51	128	111	5600	F	1.05
7125-2	0.43	127	111	8250	P	0.98
7140-1	0.47	135	132	4600	V	0.71
7140-2	0.54	137	53	6500	P	0.83
7140-3	0.51	130	100	4400	P	0.45
7150-1	0.61	152	Defective	5350	V	0.33
7150-2	0.65	151	Defective	4250	G	0.34
8050-1	0.72	51	23	5100	G	0.64
8050-2	0.67	47	17	6300	V	0.68
8050-3	0.61	44	25	5900	V	0.62
8065-1	0.52	60	24	6800	F	0.90
8065-2	0.53	52	16	7250	V	0.83
8065-3	0.53	51	36	5850	G	0.75
8080-1	0.50	81	101	5000	G	1.08
8095-1	0.49	100	107	4900	P	0.77
8095-2	0.65	102	40	6100	G	0.59
8095-3	0.49	97	30	7000	G	0.40
8110-1	0.68	106	89	4950	P	0.65
8110-2	0.55	108	25	6050	F	0.94
8110-3	0.51	109	20	7900	P	1.25
8125-1	0.43	121	157	7200	F	0.93
8125-2	0.41	120	133	7600	F	1.26
8140-1	0.51	137	144	6000	F	1.29
8140-2	0.41	137	117	8750	P	1.08
8150-1	0.73	147	53	5100	G	0.46
8150-2	0.66	143	103	4700	F	0.39

1 - See par. 2.1 in the body of the report for explanation of code
2 - Velocity of vehicle at time of skid
3 - Rubbing speed between tire and runway at time of maximum coefficient
4 - See par. 3.5 in the body of the report for meaning of "Effective Vertical Load"
5 - Quality Ratings: V-Very Good, G-Good, F-Fair, P-Poor